

Module 4: Aspects of Magnetic Recording Head

Lecture 21: Magnetic Circuits and Eddy Current losses

Objectives:

It is well known that the magnetic heads in a tape recorder or disk drive are the one of the important components of recording in a given media and playback of the signal from the recorded media. These heads have a magnetic core which either guides a concentrated magnetic field for recording (or erasing) the information or senses the magnetic flux from a recorded information in a media. For efficient recording or sensing, the understanding of magnetic circuit, selection of magnetic core materials for various types of heads, response of core materials to generate field, losses due to eddy current in various materials are very much essential. Also, with increasing the areal density in the media, the average size of the recorded bits decreases, and hence, one needs to use different types of heads for recording and sensing. Hence, the primary motivation of this module is

- (1) To understand the magnetic circuits and eddy current losses,
- (2) Selection of various types of core materials,
- (3) Magnetoresistance head,
- (4) Different types of heads (AMR, GMR, Spin valve and TMR Heads)
- (5) Disk Assembly, and general Read and Write processes
- (6) Fields from magnetic heads, and
- (7) Perpendicular recording heads.

Introduction:

Figure 21.1 shows the typical core structure of different types of heads. For the case of tape heads, the core material is either made of thin laminations of a high-permeability material stacked and cemented together or made from ferrites with a wear-resistant pole piece made from another type of magnetic alloys (Fe-Al). Each half of the core is provided with a winding of a coil. The top portion (swallow front gap) of the core generates the recording field or collects the flux from the recorded medium, while the bottom portion (back gap) offers a significant reluctance of the flux through the core. The recording of a signal is done by feeding a current representing the signal through the winding of the coil in the write head. This would generate the concentrated recording

field on the top portion of the head which lays down a permanent magnetization in the medium. The flux from this permanent magnetization of the medium induces the read voltage in the windings of the read (playback) head, when it moves close to the medium.

Magnetic Circuits:

The majority of all heads utilize a magnetic core material similar to those shown in Figure 21.1. In order to discuss various requirements, we must first introduce the concept of magnetic circuit.

It is well known that in an electrical circuit (see Fig.21.2), an electromotive force (*e.m.f*) drives a current through an electrical resistance and the magnitude of the current is given by

$$e.m.f (E) = current(I) \times resistance(R)$$

$$I = \frac{E}{R} \quad (21.1)$$

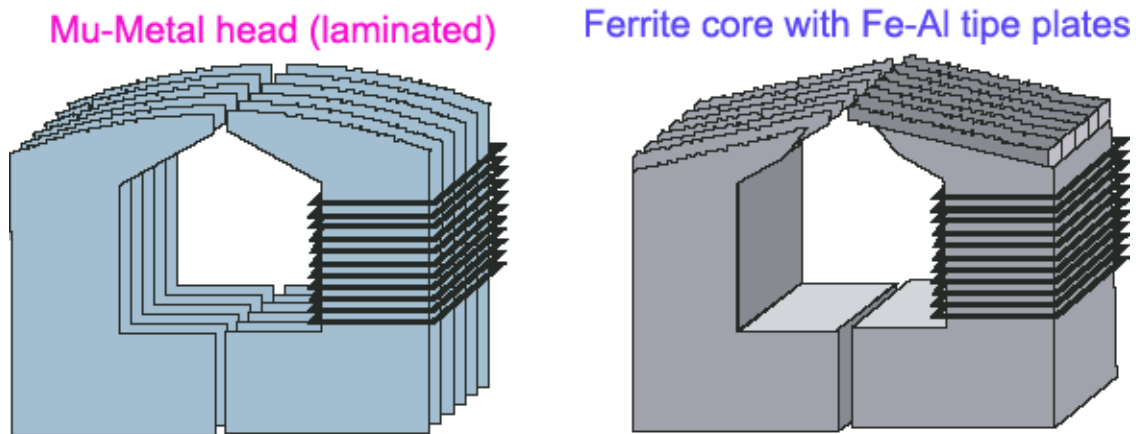


Figure 21.1: Various types of magnetic heads [1].

Similarly, in a simple magnetic circuit, as shown in Figure 21.2, a loop or core of ferromagnetic material with a relative permeability μ_r , average length L , and cross sectional area A , is wound with a coil of n turns carrying a current I , we can regard, by analogy, the coil as a source of magnetomotive force ($m.m.f$), which drives the flux ϕ through the magnetic circuit. The equation corresponding to eq.(21.1) for a magnetic circuit is

$$m.m.f = flux \times reluctance = \phi \times \mathfrak{R} \quad (21.2)$$

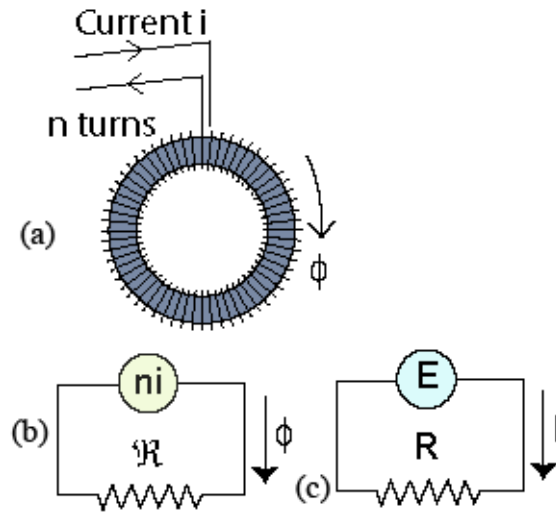


Figure 21.2: (a) A magnetic circuit and (b) equivalent circuit and (c) electrical circuit.

In this example, the $m.m.f = nI$, so that the flux in the magnetic circuit is $\phi = nI/\mathfrak{R}$. In addition, when the current I flowing through the winding, the field strength can be calculated as

$$H = \frac{nI}{L} \quad (21.3)$$

The flux through the circuit is

$$\phi = BA = \mu HA = \mu A \left(\frac{nI}{L} \right) = \frac{nI}{\left(\frac{L}{\mu A} \right)} \quad (21.4)$$

In comparison with an electrical current I passing through a wire of resistivity ρ , length L , and cross sectional area A ,

$$I = \frac{E}{R} = \frac{E}{\left(\frac{\rho L}{A}\right)} \quad (21.5)$$

The eqns.(21.4) and (21.5) clearly illustrate the analogy between the magnetic and electrical parameters:

Electrical Current (I) \Leftrightarrow Magnetic flux (ϕ)

$$e.m.f (E) \Leftrightarrow m.m.f(nI) \quad (21.6)$$

Electrical Resistance (R) \Leftrightarrow Magnetic reluctance (\mathfrak{R})

Now, let us consider a magnetic read head and the flux through the read head from the permanent magnetization of the medium, as shown in Figure 21.3.

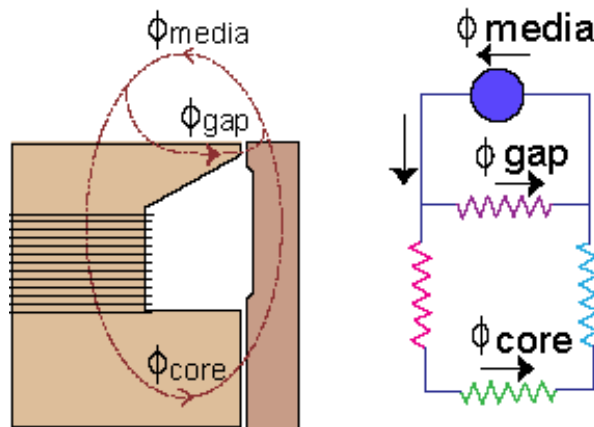


Figure 21.3: A magnetic read head and its equivalent resistance network.

The total flux in the circuit is

$$\begin{aligned} \phi_{media} &= \phi_{core} + \phi_{gap} \\ \phi_{core} &= \phi_{media} - \phi_{gap} \end{aligned} \quad (21.7)$$

Across the gap, a magnetic potential exists, which can be defined as:

$$\begin{aligned}
 V_{m,gap} &= \phi_{gap} \times \mathfrak{R}_{t,gap} \\
 V_{m,core} &= \phi_{core} \times (\mathfrak{R}_{b,gap} + \mathfrak{R}_{core1} + \mathfrak{R}_{core2}) \\
 V_{m,media} &= \phi_{media} \left[\frac{\mathfrak{R}_{t,gap} + \mathfrak{R}_{b,gap} + \mathfrak{R}_{core1} + \mathfrak{R}_{core2}}{\mathfrak{R}_{t,gap} (\mathfrak{R}_{b,gap} + \mathfrak{R}_{core1} + \mathfrak{R}_{core2})} \right]
 \end{aligned} \tag{21.8}$$

where $\mathfrak{R}_{t,gap}$ is the reluctance in the flux path from the top portion of the head, $\mathfrak{R}_{b,gap}$ is the reluctance in the flux path from the bottom portion of the head, \mathfrak{R}_{core1} and \mathfrak{R}_{core2} are the reluctance from the core materials 1 and 2, respectively. The read efficiency of the magnetic read head can be defined from the ratio of the core flux to the media flux, which is given as

$$\begin{aligned}
 \text{Read efficiency} = \eta &= \frac{\phi_{core}}{\phi_{media}} \\
 \eta &= \frac{\mathfrak{R}_{t,gap}}{\mathfrak{R}_{t,gap} + \mathfrak{R}_{b,gap} + \mathfrak{R}_{core1} + \mathfrak{R}_{core2}} = \frac{\mathfrak{R}_{t,gap}}{\Sigma \mathfrak{R}_{all}}
 \end{aligned} \tag{21.9}$$

where, $\Sigma \mathfrak{R}_{all}$ is the sum of all the reluctances going once around the circuit. Similarly, the write current can be determined from the field strength (see eqn.(21.3)) as follows;

$$\text{Write Current } (i_{write}) = \frac{H_g g}{n\eta} \tag{21.10}$$

where, g is the gap in the top portion of the head. On the other hand, the self-inductance of the winding can be determined as

$$L = \frac{n^2}{\Sigma \mathfrak{R}_{all}} \tag{21.11}$$

Note that in addition to the value of self-inductance, the magnetic circuit in a head assembly mainly determines the efficiency of the head core. The permeability of the core materials should be as high as possible. This ensures the best possible efficiency for the magnetic recording head.

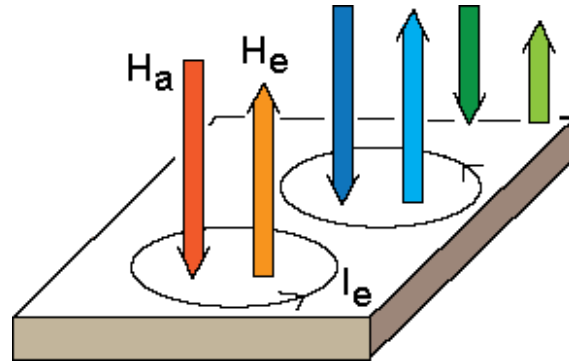


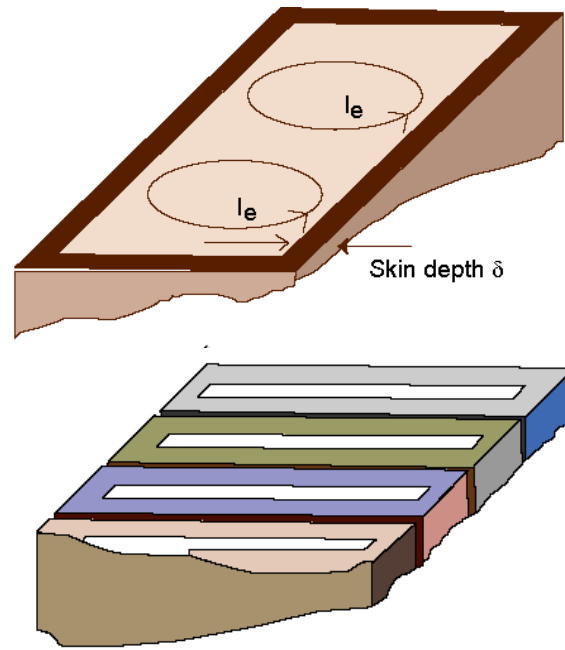
Figure 21.4: Eddy current induced in a core material by the incoming field H_a .

Eddy Current Losses:

Eddy current (also called as Foucault currents) is electric current induced in conductors when a conductor is exposed to a changing magnetic field. This is due to relative motion of the field source and conductor or due to the variations of the field with time. This can cause a circulating flow of electrons, or current, within the body of the conductor, in accordance with Lenz's law. Figure 21.4 shows how a magnetic field penetrates a sheet of conductive materials. If the applied field varies fast enough (ac field at higher frequencies) then the induced field completely oppose the outside field. This principle is mainly used in shielding. On the other hand, when the eddy current is strong enough, no magnetic field goes through the centre section of the sheet. The eddy current also increases with the frequency and hence the flux is mostly concentrated at the edges of the sheet.

The solution to this problem is to break the core up into electrically insulated laminations. Figure 21.5 shows the detail of one such lamination. If a metal alloy core of 10 cm thick is divided into 500 laminations, each 0.02 cm thick, then each lamination contains only 1/500 of the total flux. Therefore, the induced voltage around the periphery of each lamination is 1/500 of the volts/turn in the windings. On the other hand, the resistance around the periphery is equal to 250 times the resistance of the path around the entire core if it were solid. This is because the resistance is given as $R = \rho l / A$; where l is the path length around the lamination which is equal to the half of the path length around the

entire core periphery. A is the effective area which is equal to $1/500$ of the effective area around the periphery of the solid core.



Lamination increases number of surfaces.

Figure 21.5: Schematic of eddy current and magnetic flux in laminated core materials.

Neither the electric field (E) nor the magnetic field (H) penetrates far into a good conductor. Hence, they are confined at the skin of the conductor, between the outer surface and a level called the skin depth. In a good conductor, the skin depth varies as (i) the inverse square root of the conductivity and permeability.

The skin depth can be calculated from

$$\delta = \sqrt{\frac{2\rho}{(2\pi f)(\mu_0\mu_r)}} \approx 503 \sqrt{\frac{\rho}{\mu_r f}} \quad (21.12)$$

where, δ is the skin depth, μ_r is the relative permeability of the medium, ρ is the resistivity of the medium in $\Omega\text{-cm}$, f is the frequency of the current in Hz. According to eqn.(21.12), the skin depth of the materials decreases with increasing the frequency and decreasing the resistivity of the materials.

References:

[1]. F. Jorgensen, The Complete Handbook of Magnetic Recording, TAB Books; 1995

Quiz:

(1). Gold is a good conductor with a resistivity of $2.4 \times 10^{-8} \Omega\text{-cm}$ and the relative permeability is one. What is the skin depth at a frequency of 50 Hz. (Ans: 11.1 mm).

(2) What is eddy current loss?

(3) How does the read efficiency of the read head improve?

Module 4: Aspects of Magnetic Recording Head

Lecture 22: Selection of Core Materials

We have discussed the magnetic circuit and the effects of frequency and resistivity on the development of eddy currents in the core materials in the last lecture. Also, it was realized that the evolution of the magnetic heads follows the selection of core materials. Now we shall apply our understandings towards the selection of suitable magnetic materials for cores. Before, we go into the deep of the materials' properties, let us now highlight the important properties:

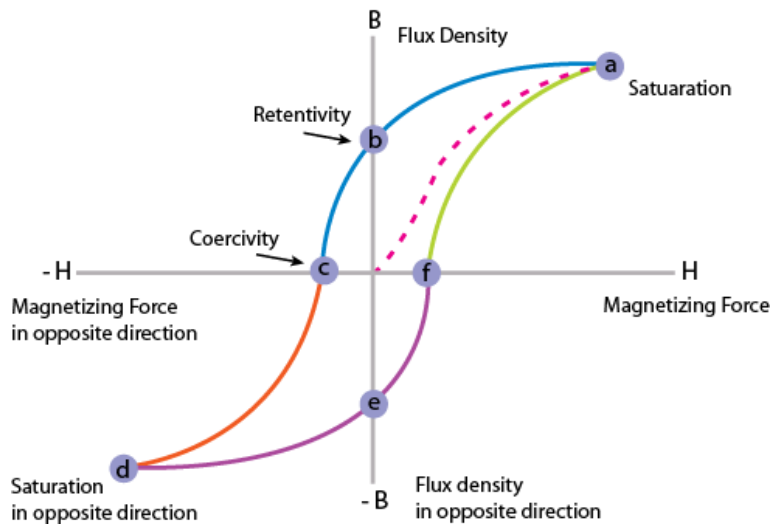


Figure 22.1: Schematic of the magnetic hysteresis loop of a ferromagnetic material.

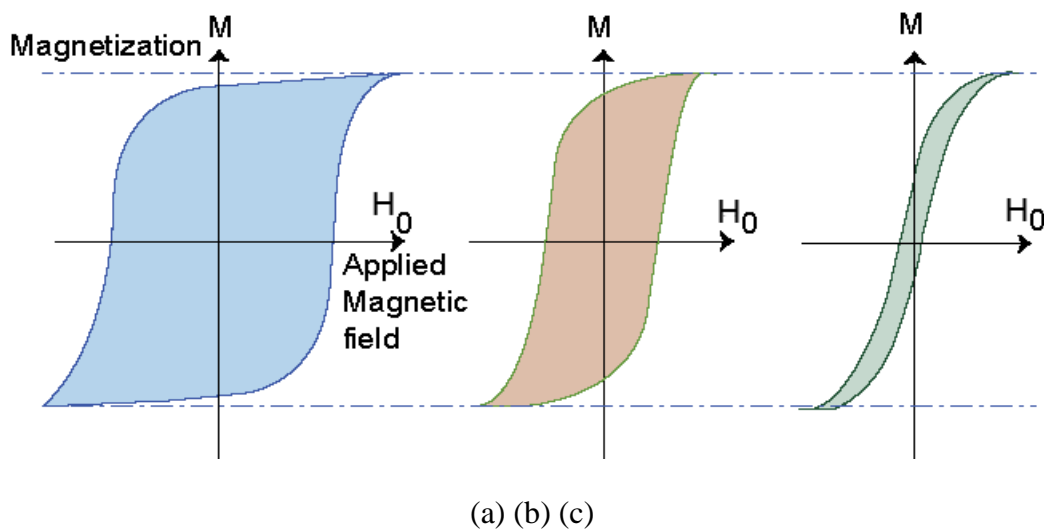


Figure 22.2: Variation in the magnetic hysteresis loops of different magnetic materials.

Figure 22.1 shows the typical magnetic hysteresis (M – H) loop of a ferromagnetic material. A great deal of information about the magnetic properties such as coercivity, permeability, retentivity, and residual magnetism can be obtained by studying its loop, which is generated by measuring the magnetic flux of a ferromagnetic material while the magnetizing force is changed continuously. Note that the hysteresis parameters are not solely intrinsic properties but are dependent on various parameters such as grain size, domain state, stresses, and temperature. Because hysteresis parameters are dependent on grain size, they are useful for magnetic grain sizing of natural samples.

There is a considerable variation in the hysteresis loop of different magnetic materials, as shown in Figure 22.2. For examples: (i) the loop, shown in Figure 22.2a, exhibits high retentivity, and high coercivity, suitable for the permanent magnets and magnetic recording and memory devices, (ii) On the other hand, the loop in Figure 2c has low coercivity, low retentivity, high permeability, and the low energy loss. These properties are desirable for the transformer and cores to minimize the energy dissipation with the alternating fields associated with AC electrical applications. Therefore,

- For efficiency → one needs materials with high permeability (μ_r)
- For low hysteresis loss → Low coercivity (H_C)
- For low eddy current loss → Low permeability, thin lamination, and High resistivity (ρ)
- Low magnetostriction coefficient
- Easy to machine and form different shapes, good durability against mechanical wear, and reasonably high hardness.

TABLE 1: Magnetic properties of various types of core materials.

Materials	μ_r	H_C (A/m)	B_{Sat} (T)	ρ ($\mu\Omega$ -cm)	T_C (K)	Composition
ToughPerm	40,000	1.6	0.5	90	553	NiFeTi
Permalloy	20,000	4	0.87	25	733	Ni ₇₉ Fe ₁₇ Mo ₄
MetGlass	20,000	0.8	0.55	130	523	FeCo
Sendust	10,000	4.8	1.0	90	773	Fe ₈₅ Al ₆ Si ₉
MnZnFerrite	4,000	8	0.55	10 ⁷	443	MnOZnOFeO
NiZnFerrite	3,000	16	0.3	10 ¹⁰	-	NiOZnOFeO
Ni-Fe	2,000-4,000	< 10	1.0	20	-	-
FeRuGaSi	1,500	40	1.4	130	-	Fe ₆₈ Ru ₈ Ga ₇ Si ₁₇

The high permeability and low hysteresis loss are achieved, when the domain walls between the magnetic domains are easily moved in magnetic materials, which should be uniform, isotropic, and free from impurities. However, a careful observation of above properties shows that the materials to have high efficiency need high permeability at low frequencies, which conflicts the requirement of low permeability materials for small eddy current losses. This can be resolved by selecting a laminated type material.

Various types of materials such as metallic alloys, metallic glasses, multilayer thin films, laminated type thin films, and ferrites, are available for the selection of core materials with optimized properties, as listed in Table 1. In this lecture, we shall briefly discuss about the different types of core materials.

Metallic Core Materials:

(1) Fe-Ni based alloys:

- Fe-Ni based alloys with low crystalline anisotropy and low magnetostriction were used in the earlier heads. The crystal direction dependent magnetostriction and crystal anisotropy in these alloys are found to be zero at a composition around 80 at.% Ni [1].
- When adding Mo in the Fe-Ni base, the initial permeability increases and triples the electrical resistivity, which resulted lower eddy current loss. They are called as Superalloy.
- Similarly, Mu-metal is obtained by adding 5 at.% Copper and 2 at.% Chromium in Fe-Ni based alloys. The high permeability (80,000 – 100,000) makes mu-metal useful for shielding against static or low frequency magnetic fields. This material is easy to roll in the form of thin sheets.
- Various types of Mu-metals (HyMu-80, HyMu-800, HyMu-800-B) were proposed as a small family of alloys by controlling the structural (microstructural parameters: grain size and grain boundaries) and magnetic properties.

(2) Fe-Al based alloys:

- The first Fe-Al based alloy was Alfenol having the composition $\text{Fe}_{84}\text{Al}_{16}$ with the moderate permeability and high saturation induction. These alloys are difficult to make as a thin sheet. Later, by altering the composition with the additional elements, the material called Sendust ($\text{Fe}_{85}\text{Al}_6\text{Si}_9$) was proposed. This is also a very hard materials and brittle in nature. However, the Sendust is used a coating materials on the gap faces, to produce a metal-in-gap (MIG) head.

(3) Metallic Glasses:

- Metallic glasses are the soft magnetic materials that are prepared using melt-spun quenching technique with a cooling rate of about 10^5 K/s. These materials have no crystalline anisotropy as the structure of the materials is completely amorphous in nature. However, the random magnetic anisotropy in these samples helps to obtain lowest coercivity and moderate saturation magnetization. Also, these materials have significantly high permeability and moderate resistivity. The ribbons are typically 10 – 50 mm wide, 20 – 50 μm thick, and are made at a rate

of 30 m/s linear velocity. The main advantage of these materials is that they can be bent and twisted without much loss in its magnetic performance.

- The primary drawbacks of these metallic core materials are frequency limitation, gap dimension inaccuracy, and mechanical softness. The frequency limitation is caused by the difficulty of making the lamination layer thinner than 30 μm . Eddy current loss, which is proportional to the thickness of materials and root of frequency, reduces the effective permeability. As a result, laminated heads are rarely used for application exceeding 10 MHz. In addition, the gap dimension inaccuracy makes it unsuitable for high areal density applications.
- One way to reduce the eddy current loss is to increase the core material resistivity. The ferrite materials have very high resistivity and significant magnetic properties suitable for core materials.

Ferrites:

Ferrites are magnetic ceramics, which play an important role in magnetic heads. Generally they are sintered materials. There are two types of materials such as Ni-Zn and Mn-Zn ferrites and have very high resistivity (four to nine order higher than the Permalloy) and considerable magnetic properties. They are formed as MOFe_2O_3 where MO is bivalent metal oxide such as MnO or ZnO with the Fe_2O_3 powder. These materials also very hard, elongating head life during head/medium contacts.

Their outstanding features are the high resistivity and reasonable good magnetic properties. This confirms that they can operate with virtually no eddy current loss at high frequencies and thus are superior to the laminated Permalloy cores. On the other hand, the major deficiency of ferrite materials is their low saturation induction values. In order to record high coercivity media, a layer of metallic alloy (Sendust) with higher saturation induction is deposited on the gap faces, which is called as MIG head.

Multilayers, Laminated materials and materials with high saturation Induction:

The other types of materials proposed for core application are multilayer materials, laminated materials and materials with high saturation induction. In the case of laminated type materials for high frequency applications, the laminations should be thin, which can be fabricated using the deposition techniques. The typical thickness involved for lamination is around 2 nm. Otherwise, the poor insulation between the core materials, stress, and coupling between the magnetic layers play a major role on determining the properties. Similarly, the eddy current damping associated with the switching of

magnetization due to domain wall or rotation process also plays a major role [2]. The multilayer films made of Fe and FeCrB also provided high-frequency cores. For example, a 10 nm Fe and 3 nm FeCrB multilayer film exhibited a high saturation induction of 1.9 T, coercivity of 40 A/m and the relative permeability of more than 2000 at 10 MHz frequency. Such multilayer films are suitable for the head with the track width smaller than 10 μm [3]. Later, Kohmoto et al proposed a large number of different kinds of alloy systems with high saturation induction of more than 10 kG [4].

With the demand for higher areal densities (150 bits/ μm^2 , bit size 40 nm, written track width = 0.15 μm), the read and write heads were developed extensively using thin film based heads, where the dimension of the heads can be controlled systematically using the lithography technique. Although the anisotropic magnetoresistance method is the first advanced method used for realizing the areal densities upto 8 bits/ μm^2 , the development of heads using giant magnetoresistance (GMR), tunneling magnetoresistance (TMR), and spin valve (SV) sensors gave a breakthrough in recording industries towards high and ultrahigh density magnetic recording. The basic principles and the development of various types of heads (GMR, TMR and SV type head) would be discussed in the upcoming lectures.

References:

- [1]. R. Hall, J. Appl. Phys. 30 (1959) 816.
- [2]. S.W. Yuan and H.N. Bertram, IEEE Trans. Magn. 29 (1993) 2515.
- [3]. Jr. R.E. Jones, C.D. Me, Recording heads, in Magnetic recording, Vol.1, Ed. By C.D. Mee and E.D. Daniel, New York, McGraw Hill, pp. 244.
- [4]. O. Kohmoto, IEEE Trans. Magn. 27 (1991) 3640.

Quiz:

- (1). What are the parameters to be considered while choosing the materials for soft core applications?
- (2). What are different types of metallic core materials available for head applications?
- (3) What are the disadvantages of choosing the ferrite materials as core materials?
- (4) What are advantages of thin film heads?
- (5) What is skin depth? How it is correlated with the eddy current losses?

Module 4: Aspects of Magnetic Recording Head

Lecture 23: Magnetoresistance Head

Magnetoresistance (MR), the change of a material's resistivity with the application of magnetic field, is a well-known phenomenon. This effect in the materials was used in the recording industry to realize the magnetic field emanating from the written information on the media. Classically, the MR effect depends on both the strength of the applied magnetic field, and the relative orientation of the magnetic field with respect to the current. There are different types of MR: Ordinary MR (OMR), Anisotropic MR (AMR), giant MR (GMR), Colossal MR (CMR), tunnelling MR (TMR), and ballistic MR (BMR), etc. However, we shall focus mainly on the basics of OMR, AMR, GMR and TMR, and the design and development of heads using the above MR techniques.

Ordinary Magnetoresistance (OMR):

OMR arises from the cycle motion of electrons in a magnetic field. For non-magnetic metals, MR effects at low magnetic field are very small, although the effect can become quite large for higher fields. The change in resistivity by the application of magnetic field is positive for all metals. Now let us focus on how the normal MR arises by a simple semiclassical argument. The force on an electron is due to the Lorentz force and the electric field:

$$F = m \frac{dv}{dt} = eE + e(v \times B) \quad (23.1)$$

and if the current density can be written as $j = \left(\frac{e}{V}\right) \sum_{i=1}^N v_i$, where V is the volume of the sample and N the number of electrons then with the relaxation time approximation we can write:

$$\frac{dj}{dt} = \frac{ne^2}{m} E + \frac{ne^2}{m} (v \times B) = \frac{j}{\tau} \quad (23.2)$$

and therefore,

$$j = \frac{ne^2\tau}{m} E + \frac{e^2\tau}{m} (v \times B) \quad (23.3)$$

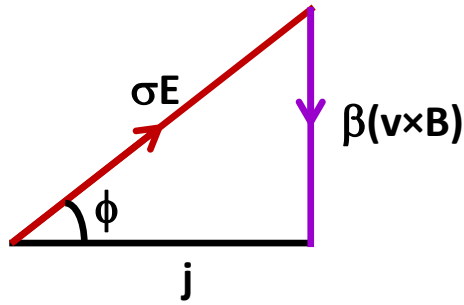


Figure 23.1. Vector diagram showing the current density, electric field, and the Lorentz force. Angle ϕ denotes the Hall angle.

This can be shown pictorially in vector format as shown in Figure 23.1, where the angle ϕ is the Hall angle. The only way to get an OMR within a free electron model is to consider a system with two types of electrons. This is often referred as a two-band model because of its application to semiconductors where the MR results from the presence of electrons and holes. Hence, we have to treat the two types of electrons, labelled 1 and 2, separately and combine the vector diagram for j_1 and j_2 . The net result of OMR is given by

$$\frac{\Delta\rho}{\rho} = (\omega_c\tau)^2 = \left(\frac{eB}{m}\tau\right)^2 = \left(\frac{ne^2\tau}{m} \frac{1}{ne} B\right)^2 \quad (23.4)$$

and simplifies to

$$\frac{\Delta\rho}{\rho} = \left(\frac{R_H}{\rho}\right)^2 B^2 \quad (23.5)$$

Where, R_H is Hall coefficient and ρ is the resistivity of the ordinary metal. As discussed earlier, the OMR is always positive and can vary in magnitude widely depending on the resistivity of the sample.

There are three different cases of OMR [1], depending on the structure of the electron orbitals at the Fermi surface:

- (a) In metals with the closed Fermi surfaces, the electrons are constrained to their orbit in k space and the effect of the magnetic field is to increase the cyclotron frequency of the electron in its orbit. The metals which exhibit this behaviour are: Al, Na, Li and In.
- (b) For metals with equal number of electrons and holes, the MR increases with H up to the highest fields measured, and does not independent of crystallographic orientations. Examples: Bi, Sb, W and Mo.

- (c) Metals that contain Fermi surfaces with open orbits in some crystallographic directions exhibits a large MR for fields applied in those directions, whereas the resistance will saturate in other directions, where the orbits are closed. Such behaviour is found in Cu, Ag, Au, Mg, Zn, Cd, Ga, Pb, and Pt.

References:

- [1]. D. Feng, G. Jin, Introduction to Condensed Matter Physics, Vol 1, World Scientific, 2005, Singapore.

Module 4: Aspects of Magnetic Recording Head

Lecture 24: Anisotropic Magnetoresistance Head

Anisotropic magnetoresistance (AMR) is the property of a material in which a dependence of electrical resistance on the angle between the direction of electrical current and orientation of the magnetic field is observed, i.e., the effect is anisotropic (see Figure 24.1).

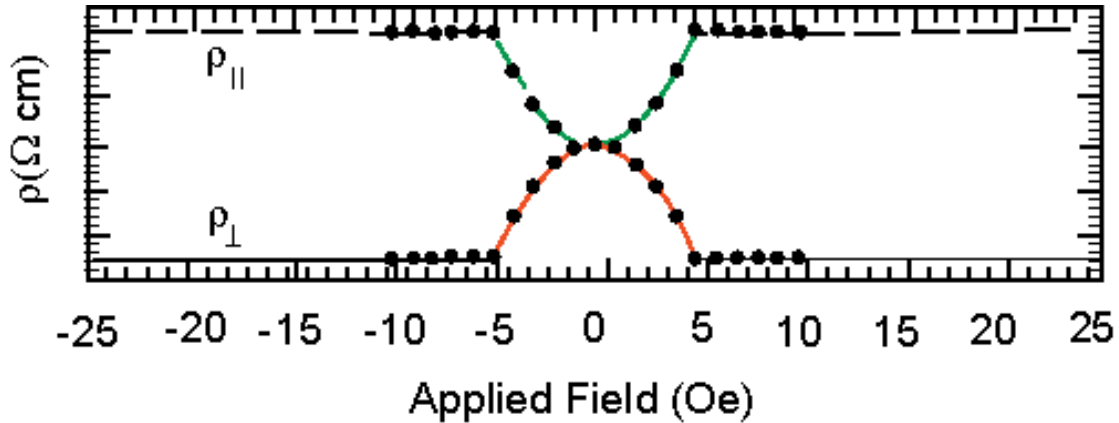


Figure 24.1: Schematic drawing of AMR for field applied parallel and transverse to the current direction.

The physical origin of the AMR is attributed to a larger probability of $s-d$ scattering of electrons in the direction of magnetic field. The electron cloud about each nucleus deforms slightly as the direction of the magnetization rotates and this deformation changes the amount of scattering undergone by the conduction electrons when traversing the lattice. The electric field due to the AMR effect is given as [1],

$$E = \rho_{\perp} j + \alpha(j \cdot \alpha)(\rho_{\parallel} - \rho_{\perp}) + \rho_H \alpha \times j \quad (24.1)$$

where j is the current density and α is a unit vector in the direction of the magnetic moment, ρ_{\parallel} and ρ_{\perp} are the resistivities parallel and perpendicular to the unit vector. The last term in eqn.(24.1) is due to the Hall electric field. Assuming that the MR is defined as the relative change in the resistivity between a fully magnetization samples and a demagnetized one, then the variation of resistance is given as

$$\frac{\Delta \rho_{\perp}}{\rho_0} = \frac{\rho_{\perp} - \rho_0}{\rho_0} \quad (24.2)$$

and

$$\frac{\Delta\rho_{||}}{\rho_0} = \frac{\rho_{||} - \rho_0}{\rho_0}$$

where ρ_0 is resistivity at zero applied field.

AMR Head element:

In the thin film of thickness T , width W , and depth D with a single domain state, the AMR effect can be described as depicted in Figure 24.2, where the resistance changed in the element can be written as

$$R = R_0 + \Delta R \cos^2\theta \tag{24.3}$$

where R_0 is the fixed part of the resistance and ΔR is the maximum change in variable part of the resistance, which is given as a function of angle in Figure 24.3.

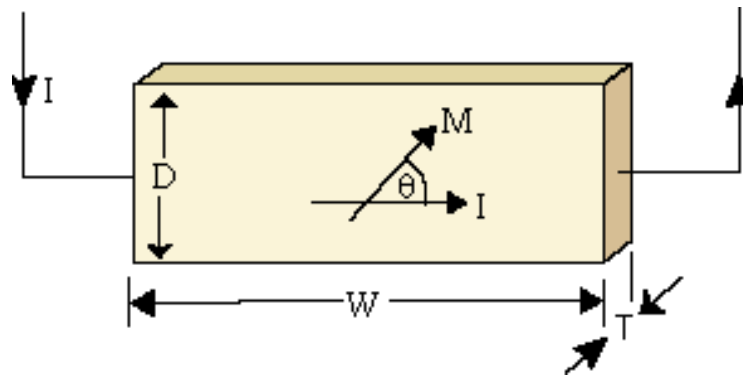


Figure 24.2: The AMR effect in a thin film with single-domain state.

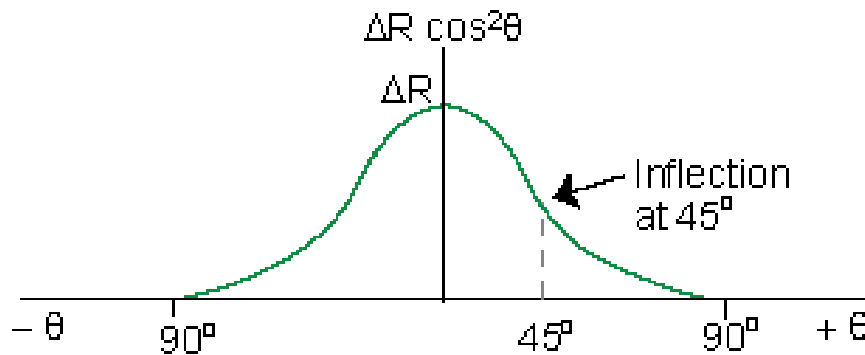


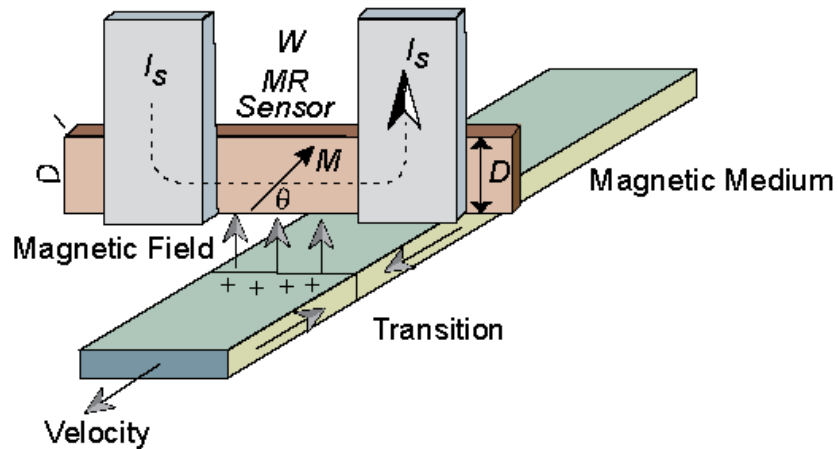
Figure 24.3: MR change in resistance versus the magnetization angle.

The basic assumption in all AMR head element is that the magnetic field produced by the written bits in the medium rotates the head element’s magnetization angle. This change in magnetization angle or biased with the proper vertical bias [2] produces a change in resistance (ΔR), which is directly proportional to small amplitude fields from the recorded medium. Hence, the output signal voltage is given as

$$\Delta V = I\Delta R = I \Delta\rho W_r / (DT) \tag{24.4}$$

where W_r is the width of the track. When the magnetization angle increases in the head element, then the magnetic poles are generated in the top and bottom regions, which generates an internal field called a demagnetization field. This demagnetization field reduces the angle, θ . Considering the demagnetization fields are negligible, the angle θ can be calculated as $\theta = \sin^{-1}(H_y/H_k)$, where H_k is anisotropy field, a field necessary to saturate the magnetization away from the easy-axis direction. As we now know the angle, θ , the eqn.(24.3) can be rewritten as,

$$R = R_0 + \Delta R \left[1 - \left(\frac{H_y}{H_k} \right)^2 \right] \tag{24.5}$$



(a)

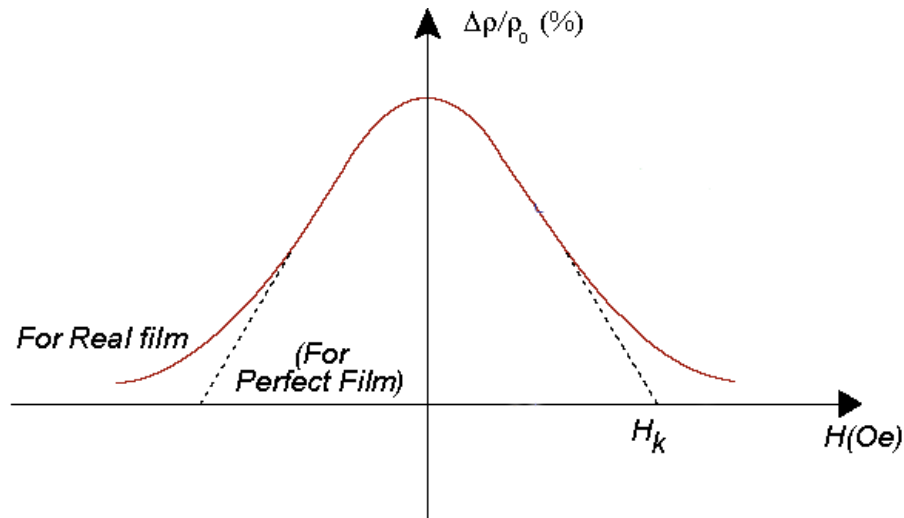


Figure 24.4: (a) Schematic drawing of the MR head, and (b) its transfer curve.

This can further be modified as

$$\rho = \rho_0 \left\{ 1 + \frac{\Delta\rho}{\rho_0} \left[1 - \left(\frac{H_y}{H_k} \right)^2 \right] \right\} \quad (24.6)$$

Here, $\Delta\rho/\rho_0$ is called as magneto-resistive coefficient, which is typically 4 % for the permalloy for the thickness larger than 1000 Å. This value is reduced to 2 % with decreasing the thickness of the films to 100 – 200 Å. Hunt [3], in 1971, proposed the concept of the MR head for the first time, as depicted in Figure 24.4. Figure 24.4a shows the schematic of the MR head and its response to the applied field (called transfer curve) is shown in Figure 24.4b. As discussed earlier, the MR head is a magnetic flux sensing device that responds to the vertical field above the recording medium averaged over the magnetic element height, D . When the current passing through the head element is kept constant, the change in resistance due to the vertical applied field (around the transition) results in a change in voltage across the head element. One of major characteristics of the MR read heads, in comparison with the inductive read heads, is that it reproduces recording signals which are primarily independent of head-medium relative speed. Note that the MR head element discussed here not only sense the vertical field resulting from the transition underneath the element, but also from the neighbouring transitions. Hence, to avoid such effects, the MR element should be shielded by the high permeability shield.

The read back voltage of a head depends on the magnetic field in the MR element from the recorded medium. This magnetic field rotates the magnetization of the MR element and if the MR element is biased at an angle θ_1 , then the read back voltage can be written from eqn.(24.4) as

$$V(\bar{x}) = I\Delta R = JW\Delta\rho_{max} (\cos^2\theta - \cos^2\theta_1) \quad (24.7)$$

where $\bar{x} = vt$ is the relative head-medium position, J is the current density, which is uniform across the MR element. It is important to understand that the values of θ and θ_1 are not uniform for the MR element, and hence the read head voltage can be represented by the average values over the film plane instead of actual values.

$$V(\bar{x}) = I\Delta R = JW\Delta\rho_{max} (\langle\cos^2\theta\rangle - \langle\cos^2\theta_1\rangle) \quad (24.8)$$

$$V(\bar{x}) = I\Delta R = JW\Delta\rho_{max} \Delta\langle\cos^2\theta\rangle$$

References:

- [1]. T.R. McGuire and R.I. Potter, IEEE Trans. Magn. 11 (1975) 1018.
- [2]. J.C. Mallison, Magnetoresistive and Spin valve heads, Fundamentals and Applications, Academic Press, CA, USA, 2002, Chap. 6.
- [3]. R.P. Hunt, IEEE Trans. Magn. 7 (1971) 150.

Module 4: Aspects of Magnetic Recording Head

Lecture 25: Giant Magnetoresistance Head

Giant MR (GMR) is a quantum mechanical MR effect observed in multilayer thin-film structures composed of alternating ferromagnetic (FM) and non-magnetic (NM) layers [1]. The effect of large MR is observed due to the significant change in the resistance depending on whether the magnetization of adjacent FM layers are in a parallel or an antiparallel orientations. This revealed that the internal moment of the electrons associated with their spin plays an important role in the transport of electric charge. The discovery of GMR triggered the field of spintronics and in 2007 the Nobel Prize in physics was awarded to Albert Fert and Peter Gurnberg for the discovery of GMR.

Resistance change in multilayer structure:

Figure 25.1 shows the typical multilayer structure consisting of a sequence of thin FM layers separated by equally thin NM metallic layer. The resistance of the magnetic multilayer is low when the magnetizations of all the FM layers are parallel (see Figure 25.1a) and the resistance become much higher when the magnetizations of the neighbouring FM layers are ordered antiparallel (Figure 25.1b).

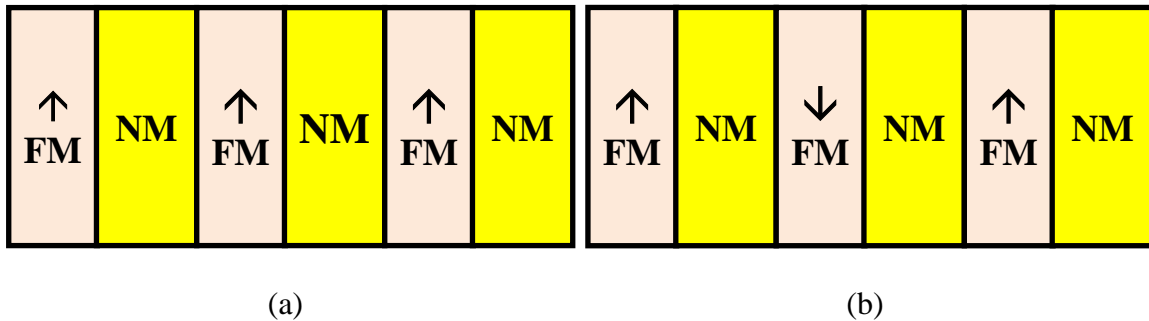


Figure 25.1: (a) Ferromagnetic and (b) antiferromagnetic configurations of magnetic multilayers film.

The definition of GMR ratio varies slightly in the literature. In order to be consistent with the AMR ratio, the definition of GMR ratio is defined as the ratio of the maximum change in resistance over the minimum resistance observed in the parallel configuration, as written in eqn.(25.1).

$$\left(\frac{\Delta R}{R}\right) = \left(\frac{R_{\uparrow\downarrow} - R_{\uparrow\uparrow}}{R_{\uparrow\uparrow}}\right) = \left(\frac{G_{\uparrow\uparrow} - G_{\uparrow\downarrow}}{G_{\uparrow\downarrow}}\right) \quad (25.1)$$

where $R_{\uparrow\downarrow}$ ($G_{\uparrow\downarrow}$) and $R_{\uparrow\uparrow}$ ($G_{\uparrow\uparrow}$) are the resistance (conductance) of the multilayer film in antiferromagnetic (AFM) and FM configurations, respectively. The most commonly used combinations of magnetic and non-magnetic layers are cobalt–copper and iron–chromium.

The GMR multilayers require a large applied field to saturate and overcome the AFM coupling of the magnetic layer to display the large GMR ratios. Interestingly, Parkin et al found that the strength of the AFM coupling is a periodic function of the NM spacer [2]. Comparison with the AMR ratio of NiFe, the field sensitivity of the GMR multilayers is considerably lower, because of the large saturation fields in the multilayers. Nevertheless, we shall focus on understanding the physical origin of the GMR and understanding the GMR using simple resistor network model.

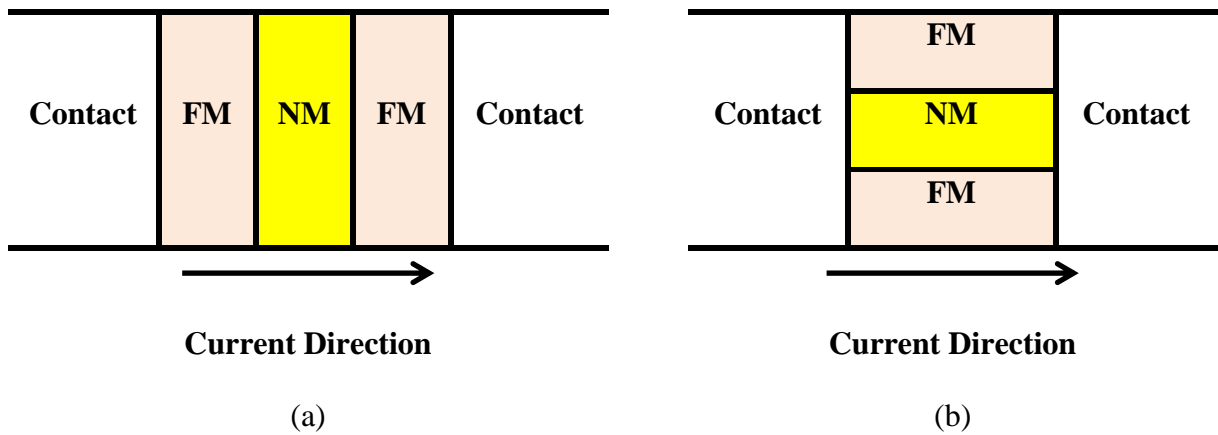
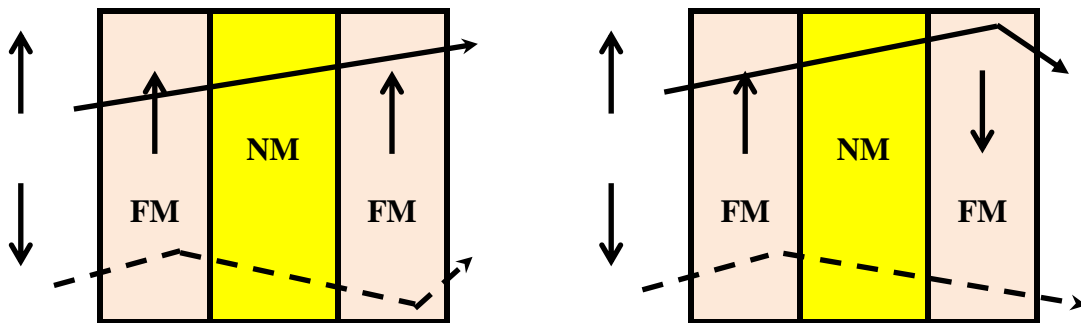


Figure 25.2: (a) Current perpendicular to plane (CPP) and (b) current in plane (CIP) GMR geometries.



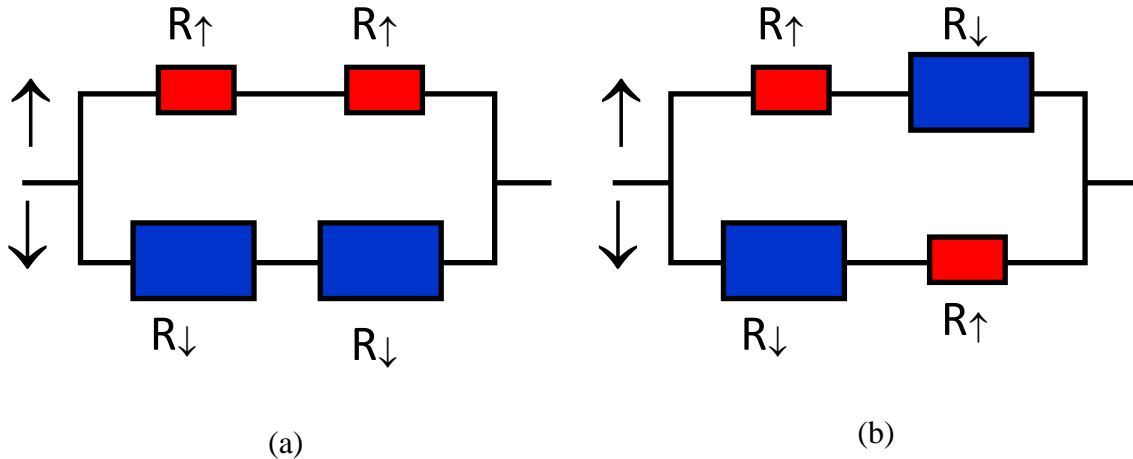


Figure 25.3: Resistor model of GMR.

Physical Origin of GMR:

There are two principal geometries of the GMR effect, which are schematically shown in Figure 25.2. In the first case (Figure 25.2a), the current flows perpendicular to the multilayers, called as current perpendicular to the plane (CPP) geometry, whereas in the Figure 25.2b, the current flows in the plane and the geometry is termed as current in the plane (CIP). Interestingly, the underlying physical mechanism is the same for both CPP and CIP geometries. Let us consider a trilayer magnetic film with two magnetic layers separated by a non-magnetic metallic spacer layer. The electron spin is conserved over distances of up to several tens of nanometers, which is larger than the thickness of a typical multilayer. Thus, we may assume that the electric current flows in two channels, one corresponding to electrons with spin \uparrow direction and the other to the electrons with spin \downarrow directions [3]. Since the spin channels are independent, they can be regarded as two wires connected in parallel. Also, when the electrons enter the FM layer, they are scattered at different rates due to directions of spin alignment (parallel and antiparallel) with respect to the magnetization of the FM layer. This is called as spin-dependent scattering.

Let us assume that electrons with spin antiparallel to the magnetization are scattered more strongly. The GMR effect in a trilayer can be now explained qualitatively using a simple resistor model shown in Figure 25.3. In the FM configuration, electrons with \uparrow spin are weakly scattered both in the first and second FM whereas the \downarrow spin electrons are strongly scattered in both FM layers. This can be simulated by two small resistors in the \uparrow spin channel and by two large resistors in the \downarrow spin channel in the equivalent resistor network shown in Figure 25.3a. Therefore, the resistance in FM configuration is determined by the low-resistance \uparrow spin channel which shorts the high-resistance \downarrow spin

channel. On the other hand, \downarrow spin electrons in the AFM configuration are strongly scattered in the first FM layer but weakly scattered in the second FM layer. The \uparrow spin electrons are weakly scattered in the first FM layer and strongly scattered in the second. This is schematically modelled in Figure 25.3b by one large and one small resistor in each spin channel. There is no shorting now and the total resistance in the AFM configuration is much higher than that in the FM configuration.

This simple resistor model of the GMR effect is believed to be correct to understand the overall behaviour. However, we need to involve a quantitative theory that can explain the differences between the CIP and CPP geometries, the observed dependence of the GMR on the layer thicknesses and also the material dependence of the effect, which is beyond the scope of the present lecture. Also, one needs to understand different types of scattering that the electrons experience in magnetic multilayer as discussed earlier in lecture 09. Typically, the scatterings due to the impurity spin at the interface, scattering from the spin waves, and strong spin-orbit interaction mix the \downarrow and \uparrow spin channels, which is detrimental to the GMR. Following the resistor network theory of GMR [4] in periodic superlattice, the change in the resistance in multilayer films can be defined as,

$$\left(\frac{\Delta R}{R}\right) = \left[\frac{(1 - \beta)^2}{4 \left(1 + \frac{N}{M\mu}\right) \left(\beta + \frac{N}{M\mu}\right)} \right] \quad (25.2)$$

Where, $\beta = \rho_{FM}^H / \rho_{FM}^L$ is a constant defined as the ratio between the low resistivity for the same (parallel) spin orientation configuration, ρ_{FM}^L , and high resistivity for the anti-parallel spin orientation configuration, ρ_{FM}^H , and $\mu = \rho_{FM}^L / \rho_{NM}$ is the ratio of the low resistivity for the same (parallel) spin orientation configuration, ρ_{FM}^L , to the resistivity of the NM layer.

The above equation helps easily to pinpoint the main factors that determine the GMR. Also, eqn.(25.2) clearly suggests that the

- (1) $(\Delta R/R)$ is a function of two variables, β and $(M\mu/N)$.
- (2) For a given value of β , GMR increases with increasing $(M\mu/N)$ values and saturates eventually.
- (3) On the other hand, the GMR value decreases with increasing the thickness of the space layer, i.e., the GMR falls as $(1/N^2)$ as shown in the Figure 25.4 for the Fe/Cr multilayers on the thickness of the non-magnetic chromium layer, described by Parkin in his original experiment [2].

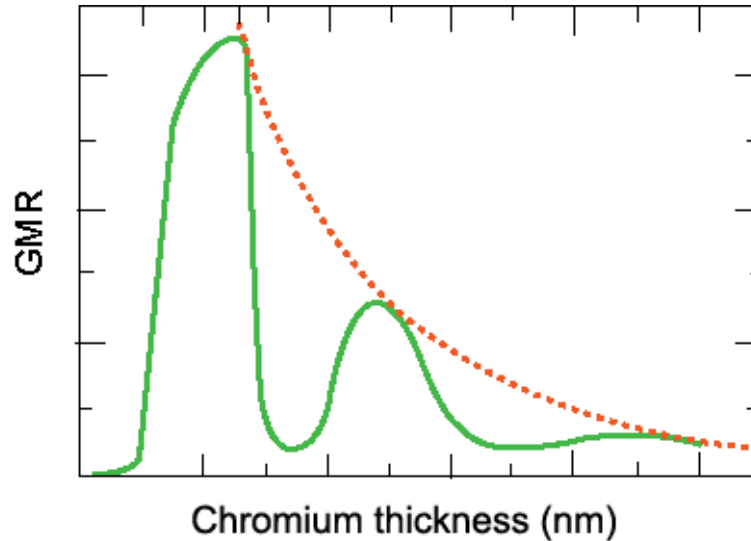


Figure 25.4: Variation of GMR ratio with the non-magnetic Cr layer thickness in Fe/Cr multilayer films. The dotted line indicates the variation as $(1/N^2)$ [2].

The oscillations of the GMR as a function of the chromium thickness occur because the MR effect is measurable only for those thicknesses of chromium for which the interlayer exchange coupling aligns the magnetic moments of all the iron layers antiparallel.

GMR Head Design:

Since the multilayer structured films, composed of alternating FM and NM layers, need a large saturation field to obtain considerably a large MR ratio, they are difficult to implement in a recording head device. This motivated the researchers to find an alternative GMR structure. Dieny et al proposed the GMR in soft ferromagnetic multilayers [5]. This multilayer structure consists of two FM layers (NiFe) separated by a NM layer (Cu) and the magnetization of the top FM layer is pinned with AFM layer (FeMn) through the exchange interaction. This arrangement helps to saturate the sample in much lower field, as the magnetic interaction between the FM and AFM layers are much weaker than that in the GMR multilayers. These GMR sandwiches are called as “Spin valves”. The details about the Spin valve structure and the GMR head using spin valve structure are discussed in the next lecture.

References:

- [1]. M.N. Baibich et al, Phys. Rev. Lett. 71 (1988) 2472.
- [2]. S.S.P. Parkin et al, Phys. Rev. Lett. 64 (1990) 2304.
- [3]. A. Fert and I.A. Campbell, J. Phys. F: Metal Physics 6 (1976) 849.
- [4]. J. Mathon, Phenomenological Theory of Giant Magnetoresistance, in Spin Electronics (Lecture Notes in Physics), Eds: M. Ziese, M.J. Thornton, Springer, New York, 2001.
- [5]. B. Dieny et al, Phys. Rev. B 43 (1991) 1297.

Module 4: Aspects of Magnetic Recording Head

Lecture 26: Spin valve based GMR Head

Spin valve based GMR has the multilayer structure similar to the GMR structure. However, the field required to switch the magnetization of the ferromagnetic (FM) layer in the GMR multilayer is small, as the interaction between the FM layer is much weaker than that in the GMR multilayer. In this lecture, we will discuss about the various types of spin valve structures, their functions, and the basic design of GMR heads.

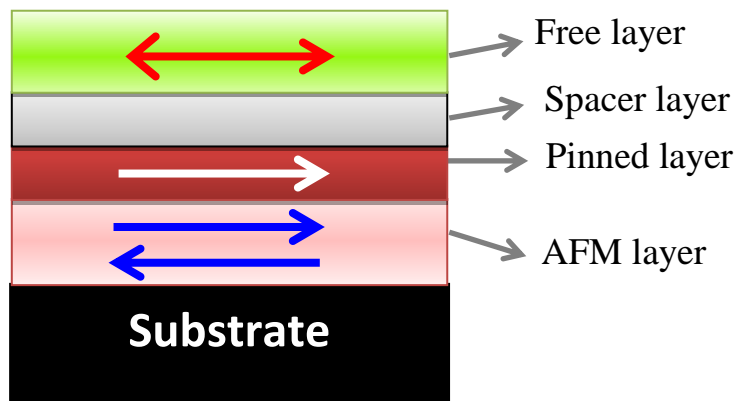


Figure 26.1: Schematic arrangement of bottom spin valve structure.

Types of Spin values:

The typical spin valve GMR based read head, introduced by IBM in 1997, consists of four layers, as shown in Figure 26.1:

1. A layer of FM material that is closest to the surface and acts as a sensor. This is called as free layer, because the direction of its magnetization switches to align with the particular bit of the recorded medium.
2. A spacer layer of non-magnetic (NM) serves as a buffer between the two magnetized layers.
3. A pinned layer, that has a fixed, unchanging magnetic orientation.
4. An exchange layer of a material that insulates the pinned layer from outside magnetic fields.

The above spin valve is called as bottom spin valve, as the bottom FM layer (pinned layer) is pinned with the adjacent AFM layer, while the top FM layer is free to rotate. The other types of spin valves such as top spin valve and symmetrical spin valve structures are shown schematically in Figure 26.2. In the case top spin valves, the top FM layer is pinned and the bottom FM layer is free to rotate. In the symmetrical spin valve, the central FM layer is free, while the other two FM layers are pinned. This arrangement results higher GMR ratio than the bottom spin valve because it contains more spin dependent scattering interfaces.

Note that in addition to these four layers, various types of underlayer, seed layer, and cover layers are used to promote desirable film texture, morphology, control of the interfacial spin dependent scattering and surface coating.

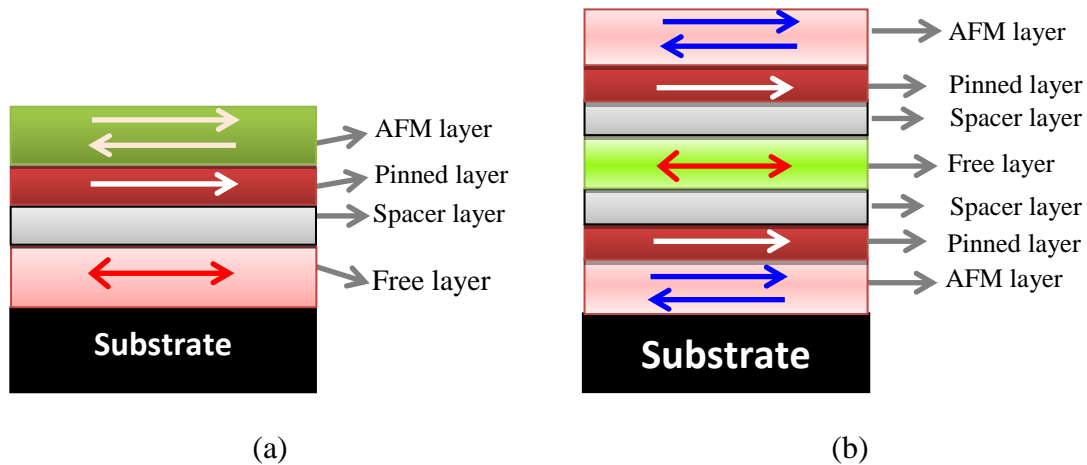


Figure 26.2: Schematic arrangement of (a) top and (b) symmetrical spin valve structures.

Pinning Method and Materials:

In order to pin one of the FM layer, various methods were employed by employing different types of pinning. The commonly used pinning methods include:

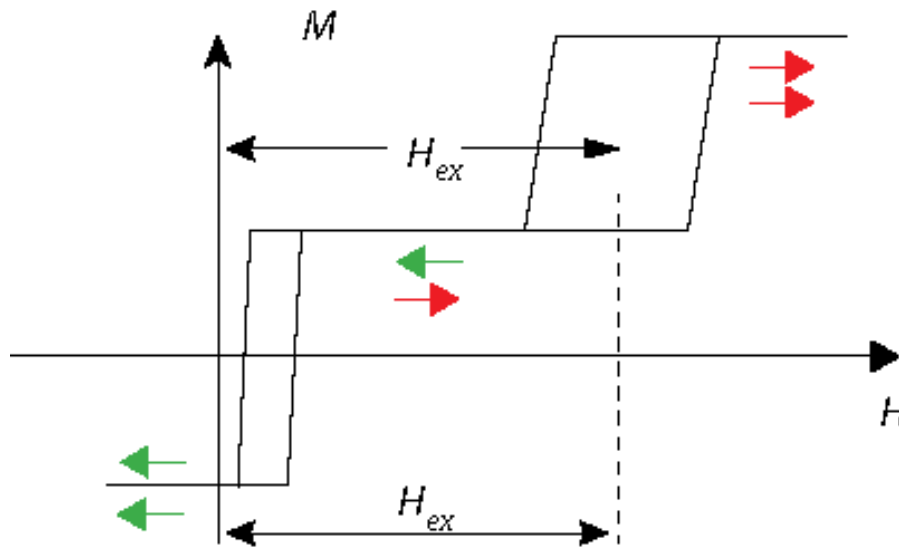
- (1) AFM or ferromagnetic exchange bias layer (NiO, NiMn, IrMn, PtMn, etc.),
- (2) Permanent magnetic thin film layer (CoCrPt, CoSm, etc.),
- (3) Synthetic AFM layers (SAL, Co/Ru/Co), where the two FM layers separated by a thin NM layer produce a AFM coupling as observed in GMR multilayers.

Figure 26.3 shows the typical magnetic hysteresis ($M - H$) loops and the corresponding magnetoresistance (MR) transfer curve of a spin valve structure. It is clear from the figure that there are two hysteresis loops: One is close to the origin and the other one is considerably away from the origin. This suggests that the $M - H$ loop close to the origin is associated with the magnetic switching of the free layer, while the other loop is associated with the magnetic switching of the pinned layer. Note that the $M - H$ loop of the free FM layer shifted away from the origin mainly due to the considerable exchange coupling between the free FM and pinned layer. The resistance in the curves shows initially minimum value and rises to a maximum and falls back to minimum at higher fields. This confirms that the resistance of the spin valve is a maximum when the top and bottom layers are antiparallel and minimum when parallel.

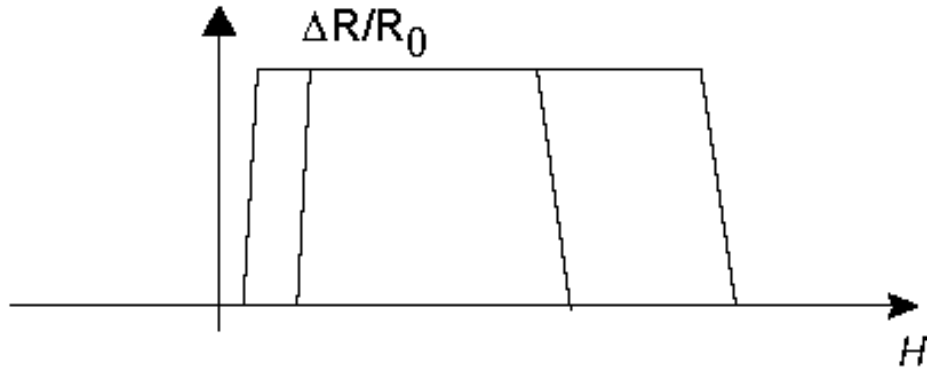
The GMR ratio in the spin valve is defined as

$$\left(\frac{\Delta R}{R_0}\right) = \frac{\Delta R_{max}}{R_0} \left[\frac{1 - \cos(\theta_2 - \theta_1)}{2} \right] \quad (26.1)$$

where θ_1 and θ_2 are the magnetization orientation angle of the pinned and free FM layers in the spin valve, respectively.



(a)



(b)

Figure 26.3: (a) The magnetic hysteresis loop and (b) MR transfer curves of a spin valve along the easy axis. The arrows represent the magnetization of free and pinned FM layers.

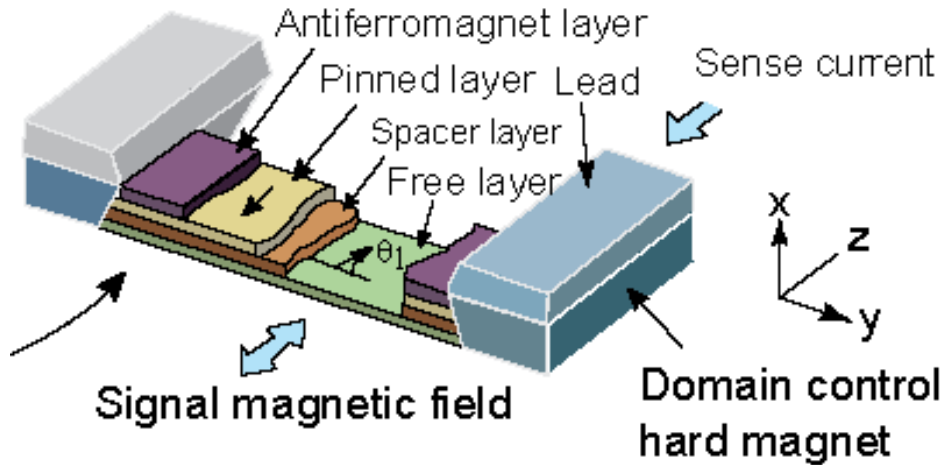


Figure 26.4: Schematic diagram of spin valve head [1].

Spin valve GMR Head Design:

GMR heads, reported by various companies [2-4], are capable of reading the areal densities larger than 5 Gbits/in². Figure 26.4 shows the typical spin valve based GMR head, where the free layer magnetization can rotate from 0° to 90°. The read back voltage from a spin valve GMR read head is

$$V_{GMR}(\bar{x}) = I\Delta R_{max} \left(\frac{-\cos(90^\circ - \theta_1) + \cos(90^\circ - \theta_2)}{2} \right) \quad (26.2)$$

where I is the sense current through the spin valve, and the angle θ_2 is the sluggish magnetization orientation of the free layer. The eqn.(26.2) can be rewritten as,

$$V_{GMR}(\bar{x}) = \frac{1}{2} I \Delta R_{max} [\langle \sin \theta_1 \rangle - \langle \sin \theta_2 \rangle] \quad (26.3)$$

It is important to realize that the GMR head output voltage is almost 8 times larger than the AMR head, when the sense current and the trackwidth are the same for both types of heads. This indirectly suggests that the GMR heads could generate greater signals compared to conventional AMR heads. Also, this would help to reduce the trackwidth by keeping the required amount of signal for readback, which indicates that the GMR heads can be used for the magnetic recording with the areal densities up to 10 Gbits/inch². However, for areal densities >10 Gbits/inch², the discovery of alternative heads or large improvement in GMR based heads is necessary. So the question arises now is that what types of heads would be suitable for the areal densities >10Gbits/in²? This question opened up a considerable interest among the scientist for the development of new types of heads.

References:

- [1]. FUJITSU Sci. Tech. 37 (2001) 2.
- [2].H. Kanani et al, IEEE Trans Magn 32 (1996) 3368.
- [3]. H. Yoda et al, IEEE Trans Magn 32 (1996) 3363.
- [4]. C. Tsang et al, IEEE Trans Magn 30 (1994) 3801.

Module 4: Aspects of Magnetic Recording Head

Lecture 27: Tunnelling Magnetoresistance Head

Moodera et al [1] proposed the room temperature spin-dependent tunnelling in a trilayer structure, consisting of a two ferromagnetic (FM) layers separated by a thin insulator, as depicted in Figure 27.1. When the insulator barrier is thin enough, the electrons can tunnel through the insulator from one of the FM layer to another or vice versa. In this scenario, the tunnelling current through the insulator is larger when both the FM layers are aligned parallel than when they are aligned antiparallel. This is called tunnelling magnetoresistance (TMR) effect.

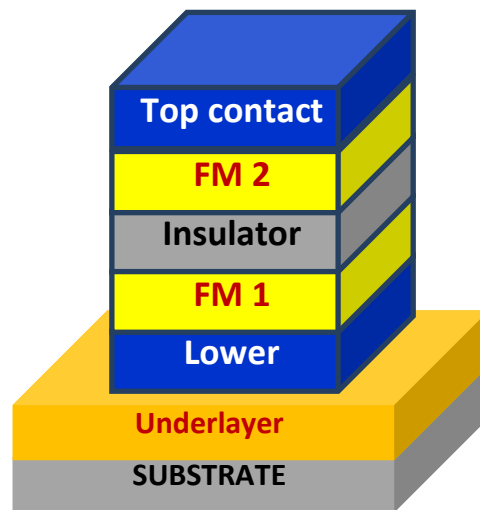


Figure 27.1: Schematic presentation of a multilayer structure in TMR.

In such case, the TMR can be written as

$$\left(\frac{\Delta R}{R}\right) = \left(\frac{R_{\uparrow\downarrow} - R_{\uparrow\uparrow}}{R_{\uparrow\uparrow}}\right) = \left(\frac{G_{\uparrow\uparrow} - G_{\uparrow\downarrow}}{G_{\uparrow\downarrow}}\right) \quad (27.1)$$

where $R_{\uparrow\downarrow}$ ($G_{\uparrow\downarrow}$) and $R_{\uparrow\uparrow}$ ($G_{\uparrow\uparrow}$) are the resistance (conductance) of the multilayer film in antiferromagnetic (AFM) and FM configurations, respectively.

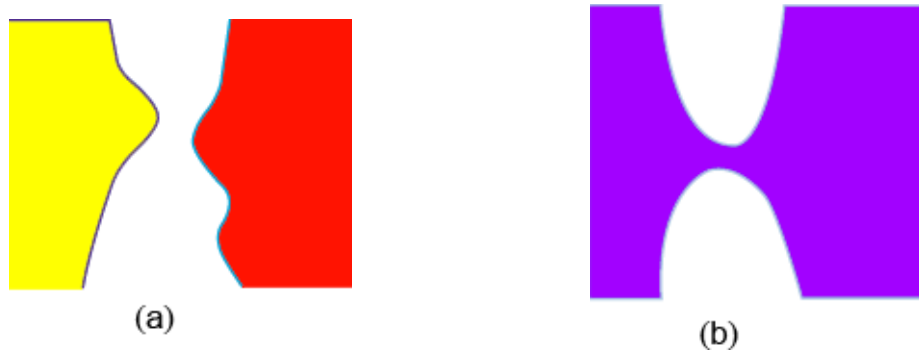


Figure 27.2: Schematic representations of a (a) tunnel junction and (b) contact junction.

So, the TMR structure is similar to GMR, except the fact that the metallic non-magnetic (NM) layer in GMR is replaced by an insulator in TMR. Hence, TMR is another subject of great interest. The spin dependent tunnelling poses many interesting challenges, but the number of applications for the magnetic tunnel junctions continues to grow [2]. Hence, it is essential to understand the physics behind the effect of magnetic fields on the current tunnelling through the magnetic junctions and to obtain the suitable equation to describe the TMR.

Magnetic Junctions:

The transport between two metallic electrodes can be in general classified into two types as displayed schematically in Figure 27.2: One type of junction is tunnel junction, where the separation between the electrodes varies from few to few tens of angstroms and the other is a contact type, where the contacts are made at some points selectively.

(1) When the separation between the electrodes exceeds a few angstroms, electrons move between them through tunnelling. The probability that any one electron tunnels through a barrier of height V and length l is given by:

$$\tau = \exp \left[-cl \sqrt{\frac{2mV}{\hbar^2}} \right] \quad (27.2)$$

where c is a constant of order unity, which depends on the detailed shape of the barrier and on the electronic wavefunctions. The barrier can be either (i) the vacuum created between the two electrodes, in which case the height of the barrier is given by the work function of the electrodes, or (ii) by inserting an insulating layer between the two electrodes, as shown in Figure 27.1. The barrier height in the latter case depends on the position of the edges of the gap of the insulating material with respect to the Fermi level of the electrodes. It is clear from the eqn.(27.2) that the tunnelling depends exponentially on the distance between the electrodes, and we may expect that in a junction of macroscopic size, the current will be due to tunnelling events at bulging of the interface. A change of a few angstroms even can greatly modify the tunnelling probability. The conductance at any of these points is given by:

$$g \sim \frac{e^2}{h} \tau \sim \frac{e^2}{h} \exp \left[-cl \sqrt{\frac{2mV}{\hbar^2}} \right] \quad (27.3)$$

(2) On the other hand, the two electrodes can be in contact in some points. Then, the conductance of each contact is given by e^2/h times the number of electron channels through the contact. It is roughly given by the cross section of the contact expressed in units of inverse square Fermi wavevector (k_F^{-2}). Then,

$$g \sim \frac{e^2}{h} k_F^2 A \quad (27.4)$$

where A is the area of the junction.

TMR Effect:

Note that we have not considered the magnetic properties of the electrodes in the above discussion. If the number of electrons of the two spin polarizations is not equal, we must define a spin dependent conductance, at each of the points where electrons move from one electrode to the other. The expressions defined earlier are modulated by the density of states of each type of electrons. For a given bias voltage V , the electrons which participate in the conduction come from the levels located, at most, at a distance eV from the Fermi energy, E_F . Thus, in order to understand the transport at small bias voltages we need to know density of states at the Fermi level, $D_{\uparrow}(E_F)$ and $D_{\downarrow}(E_F)$. As discussed earlier, the tunnelling magnitude will be spin dependent, as shown in Figure 27.3.

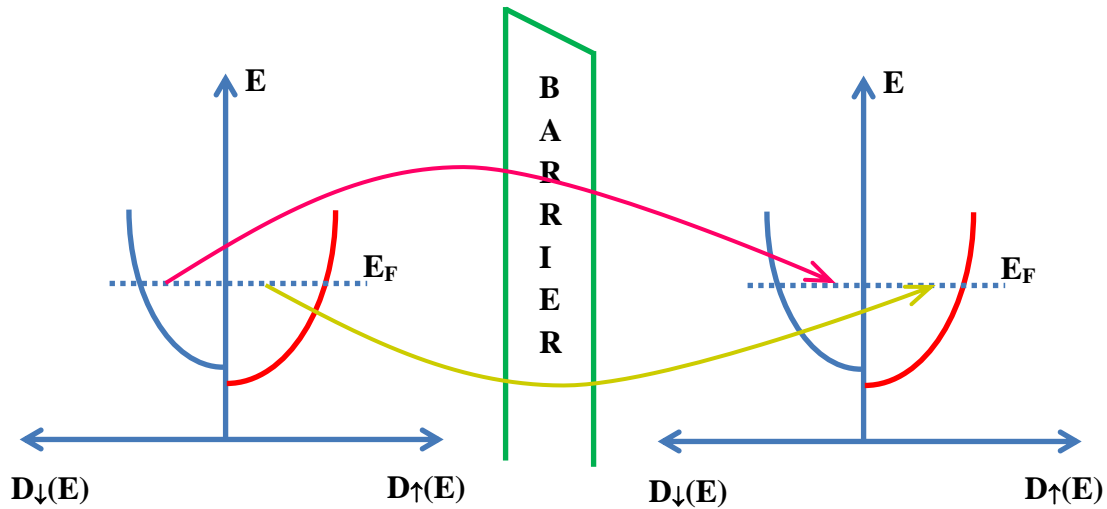


Figure 27.3: schematic drawing of spin dependent tunnelling in FM/NM/FM junctions.

As the applied magnetic field modifies the polarization of the electrodes, the density of states also changes significantly. Further, the barrier can be described in terms of an energy dependent transmission coefficient. To simplify the calculation, the direct magnetic coupling between the electrodes is negligible and the orientation of the magnetization in each electrode will be determined by bulk effects. This helps to assume that the relative orientation of the magnetization of the two electrodes can take any value. Therefore to calculate the magnetoresistance (MR) of the tunnel junction, we just need to compare the conductance with a random orientation of the magnetization of the electrodes and that when both magnetizations are aligned. Further, we assume that

$$\begin{aligned} D_{\downarrow}(E_F) &\propto N_{\downarrow} \\ D_{\uparrow}(E_F) &\propto N_{\uparrow} \end{aligned} \quad (27.5)$$

where N_{\downarrow} and N_{\uparrow} are the number of electrons with down and up spin. Subsequently, in the unpolarized situation, we may expect that

$$\begin{aligned} G_0 &\propto \frac{1}{2} (N_{\uparrow L} N_{\uparrow R} + N_{\uparrow L} N_{\downarrow R} + N_{\downarrow L} N_{\uparrow R} + N_{\downarrow L} N_{\downarrow R}) \\ &= N_L N_R \end{aligned} \quad (27.6)$$

where the indices L and R stands for the left and right electrodes, and N_L and N_R are the total number of electrons. On the other hand, in the polarized case, we have:

$$G \propto N_{\uparrow L} N_{\uparrow R} + N_{\downarrow L} N_{\downarrow R} \quad (27.7)$$

Hence, we have

$$\frac{\Delta G}{G_0} = \frac{G - G_0}{G_0} = \frac{(N_{\uparrow L} - N_{\downarrow L})(N_{\uparrow R} - N_{\downarrow R})}{N_L N_R} \quad (27.8)$$

The eqn.(27.8) clearly indicates that the MR is directly proportional to the polarization of the electrodes. This simple analysis roughly explains the pioneering experiments in spin tunnelling [3,4]. On the other hand, a more realistic theory includes two additional effects:

- (1) The density of states at the Fermi level needs not be proportional to the total polarization.
- (2) The wavefunctions of the majority and minority electrons near the barrier need not be the same. Then, the transmission coefficient acquires a spin dependence, which influences the MR.

The TMR effect can also be demonstrated, if the spin polarization of the electrodes involved in the multilayer films is known [5]. Assuming the spin polarization of the two electrodes as P_1 and P_2 , the relative resistance change is given as,

$$TMR = \frac{\Delta G}{G_0} = \frac{2P_1P_2}{1 - P_1P_2} \quad (27.9)$$

The major challenges to use the spin dependent tunnel junctions in magnetic read heads are to reduce the junction resistance and optimize the multilayer structure for obtaining high TMR. The lowest junction resistance area reported to date is about $0.2 \text{ k}\Omega\text{-}\mu\text{m}^2$, which is approaching close to the required values for MR read head applications [6]. Also, a large TMR of up to 600 % at room temperature and more than 1100 % at 4.2 K were observed in junctions of CoFeB/MgO/CoFeB [7], which is sensitive to the composition of the CoFeB [8]. This suggests that the research on spin dependent tunnelling is rapidly developing and more exciting results are expected in the future from the application point of view.

References:

- [1]. J.S. Moodera et al, Phys. Rev. Lett. 74 (1995) 3273; J. Appl. Phys. 79 (1996) 4724.
- [2]. R. Meservey and P.M. Tedrow, Phys. Rep. 238 (1994) 173.
- [3]. M.H. Devoret and H. Grabert, "Single Charge Tunneling", Plenum Press, New York (1992).
- [4]. J. M. D. Coey, A. E. Berkowitz, et al, Phys.Rev. Lett.80 (1998) 3815.
- [5]. M. Julliere, Phys. Lett. A 54 (1975) 225.
- [6]. H. Tsuge et al, Res. Soc. Symp. Proc. 517 (1998) 87
- [7]. S. Ikeda et al, Appl. Phys. Lett. 93 (2008) 082508.
- [8]. M. Kodzuka et al, J. Appl. Phys. 111 (2012) 043913.

Module 4: Aspects of Magnetic Recording Head

Lecture 28: DISK Drive Assembly, Writing and Reading process

The evolution of rigid disk drive began in 1956 after the introduction of the IBM Drive, the 350 RAMAC, which is the hybrid of a digital tape recorder and phonograph. The size of the IBM RAMAC was approximately the size of two refrigerators and stored only 5 Megabit characters in a stack of 50 discs. The development of hard disk took place in slow pace up to 1990. Later Western Digital and IBM introduced the disk drives with the thin magnetoresistive (MR) heads, which stores about 1 GB. Over last two decades, the discovery of GMR heads and spin valve based heads boosted the hard disk industry to fabricate high storage space drives for various applications towards consumer electronics. Due to the constrains from the natural limits (superparamagnetic effects) in the longitudinal magnetic recording, the new recording technology based on the perpendicular magnetic recording was introduced by Toshiba in 2005. In 2006, Seagate released one of the largest hard disk drives Barracude 7200 with 750 GB areal density, while the largest capacity drives up to 4 Terabytes were introduced by Seagate. Figure 28.1 shows the photographic view of the parts of the recent disk drive.



Figure 28.1: Photographic view of the hard disk drive [1].

The disk drive parts and their functions are given in the list that follows:

1. Since the purpose of the hard disk is to store data and retrieve it reliably over a long period, the hard disk medium should be fabricated on a rigid platform to avoid any damage. This platform along with the deposited films for recording is called as platter.
2. The platters are fixed on spindle, which rotates at a speed varying from 1800 revolutions per minute (rpm) to ~10000 rpm, i.e., the relative velocity between the head and the disk is about 40 m/sec.
3. The head writes and reads data from the disk.
4. The head is located at the end of the actuator arm and it is a part of the slider, which has a flexible connection to the actuator, and it has a profiled surface facing the medium that forms an air-bearing surface allowing the head to hover at a close distance of about 10 – 100 nm from the medium.
5. Also, the actuators provide a means of moving the head/slider from one track to another and produce motions to retain the head in the center of the track.

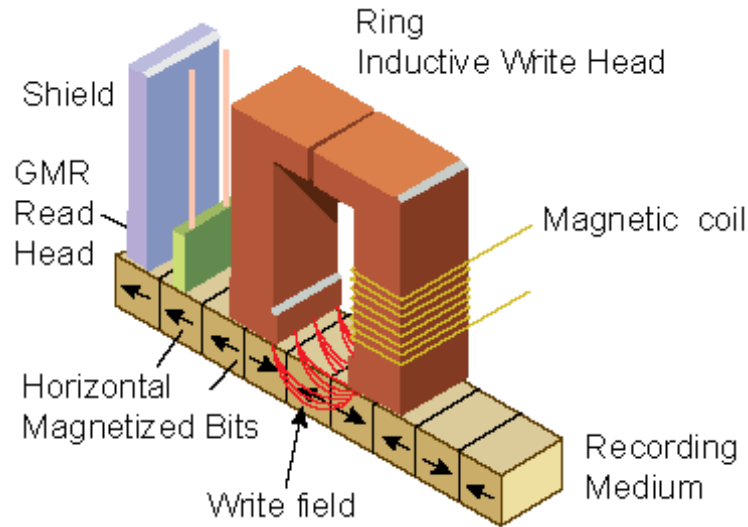


Figure 28.2: Schematic drawing of ring head and disk [2].

Writing and Reading Process:

Figure 28.2 shows a schematic representation of a ring head and a disk. The head consists of a ring or yoke of magnetic material with a coil of wire wrapped on the core. The coil is connected to the channel electronics. There is a gap of about 10 – 100 nm between the bottom of the head and recording medium. The data is written in the medium with the following sequences:

1. The channel in the electronics part of the disk receives data to be stored from the computer, and after some processing, it generates the currents in circuits called write drivers.
2. Subsequently, the write driver supplies current to the head coil.
3. Now, the coil current results in magnetization of the "core" of the head.
4. Then the magnetic field spreads out in the gap between the head and disk.
5. The fringe field from the head reaches the medium and magnetizes it in one of the two possible directions as shown in Figure 28.2. Note that only the horizontal component of the fringe field is used for writing the information in the case of longitudinal magnetic recording.

The current in the coils is changed depending on the changes in the data and coding rules. This would result a change in the direction of the field near the gap and reversing the magnetic poles in the medium accordingly. By this process, the sequence of data from the channel electronics gets translated into medium as the magnetized poles.

During the reading process, the write drivers are typically switched off and virtually isolated from the head coil. Then, the reading preamplifier is connected to the head and the following sequence of events or reading converts the magnetized poles in the medium into bits.

1. As the head passes near the recorded medium within a reasonable height, the fringe field from the magnetic pole enters the core and the core of the head becomes magnetized.
2. The direction of magnetization of the core will certainly depend on the direction of the magnetization of the medium.
3. The change in magnetization in the core results in a voltage across the head coil.

According to Faraday's law, $V = -d\phi/dt$ is generated if the flux changes with time. Particularly, at the transitions where the magnetization in the medium change the voltage is generated in the coil. Depending on the data stored in the media, there are two types of transitions possible: (1) north poles facing north poles and (2) south poles facing south poles. These transitions create positive- or negative-going voltage pulses in the head coil, which is further amplified after a series of detection steps, results in the usable data to the computer processor.

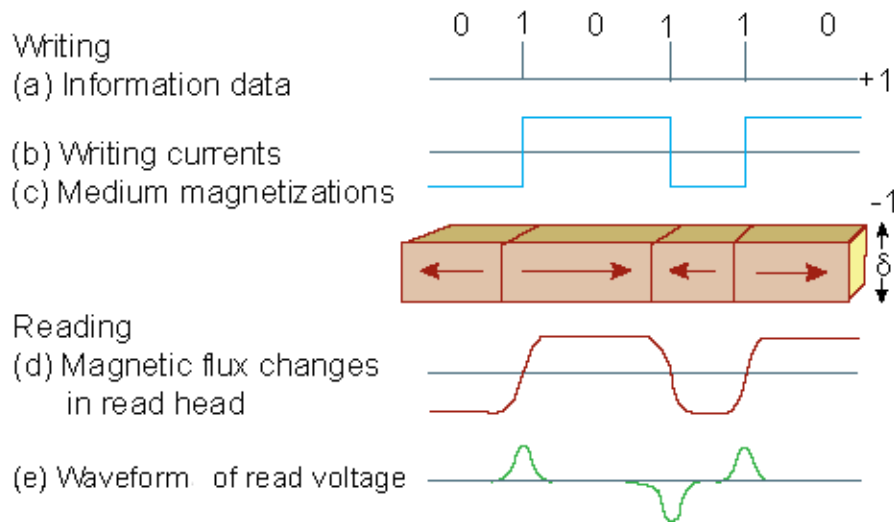


Figure 28.3: Sequences of writing and reading data in disk using heads.

A typical write and read sequences are depicted in Figure 28.3 [3]. Figure 28.3a shows a sequence of data received from the computer in the form of a series of 1 and 0. In the given sequence of the data, the current through the head coil must reverse at each 1 state and not reverse at each 0 state as shown in Figure 28.3b. When this is done during disk rotation, the magnetization of the recorded bits in the disk medium looks as in Figure 28.3c. This is how the writing is done in the disk medium. Assuming that the given sequence is written in the disk, we shall try to understand the reading process. When the head passes through the written bits, a small change in the yoke magnetization occurs, as depicted in Figure 28.3d. This develops a voltage in the coil as displayed in Figure 28.3e. This occurs each time a transition between the bits passes under the head.

Note that for writing, one needs current on the order of few tens of milliamperes, so that the writing field at the disk medium is high enough to write the bits. On the other hand, for reading, the induced voltages in the head are in the range of millivolts, which requires a complex external detection and amplification to extract usable data out of such low signals. Nevertheless, the primary theme of the hard disk technology lies in its ability to store data indefinitely without power, and retrieve it inexpensively and reliably.

References:

- [1]. General instructions on hard disk drive.
<http://news.bbc.co.uk/2/hi/technology/6677545.stm>.
- [2]. Writing and Reading Data in Magnetic recording process
<http://www.birmingham.ac.uk/research/activity/metallurgy-materials/magnets/background/magnetic-recording.aspx>.
- [3]. R. M. White, Introduction to Magnetic Recording, IEEE, 1985.

Module 4: Aspects of Magnetic Recording Head

Lecture 29: Reading and Writing process

In the earlier lectures, we have discussed briefly about the writing to and reading the data from the disk medium. As the writing and reading processes are the core parts of the magnetic recording, we shall discuss for a quantitative understanding of the factors involved for the above processes so that the general design as well as the recent development can be understood.

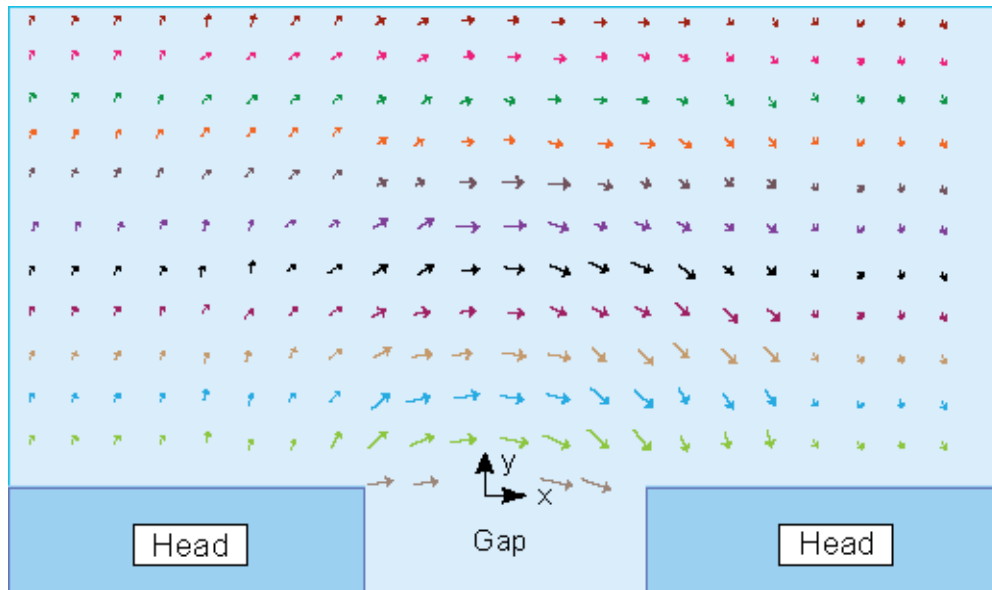


Figure 29.1: Schematic drawing of the head field [1,2].

Field from the head:

As we know well that a sufficient writing field (more than the coercivity of the medium) must be provided to the disk medium to write magnetic transitions. Otherwise, the applied field close to or just below the coercivity reverse only half the magnetization due to the non-square nature of the hysteresis loops. Hence, in general, the applied field of 2 to 3 times the coercivity of the materials should be applied to reverse all the magnetization. Note that a factor of 2.5 is commonly used in the recording process. Figure 29.1 displays the stray fields near the gap of the inductive head. While the direction of the arrow indicates the direction of the magnetic field, its length indicates the magnitude of the field strength. The arrow directions are horizontal at the center of the gap above the gap center. However, the direction of the arrow changes at various angles with respect to the horizontal axis when we move in both directions away from the center. A careful observation of the picture suggests that the contour is circle. According to the Ampere's

law, the magnetic field surrounding a straight conductor carrying current I is radially distributed, and the field is given as $I/(2\pi r)$, where r is the radius of the circular path. Following the above view and considering the head gap is small and the contour is circle, the field at a distance r can be determined as $nI/\pi r$ A/m. Here, n is the number of coil turns and πr represents the integration of field over the semicircle.

For longitudinal magnetic recording, the interest is to calculate the field along the horizontal direction at a particular gap between the head and medium. The general equations for the x and y fields of a ring head of infinite poles derived by Karlqvist [1] are turn out to be,

$$H_x(x, y) = \frac{H_g}{\pi} \left(\tan^{-1} \left(\frac{x + g/2}{y} \right) - \tan^{-1} \left(\frac{x - g/2}{y} \right) \right)$$

$$H_y(x, y) = \frac{-H_g}{2\pi} \ln \left[\frac{\left(\left(x + \frac{g}{2} \right)^2 + y^2 \right)}{\left(\left(x - \frac{g}{2} \right)^2 + y^2 \right)} \right] \quad (29.1)$$

where g is the head gap, H_g is the magnetic field strength inside the head gap due to the current in the coil. The complete derivation of the above equation by using various assumptions can be found in module 3 [1]. The eqn.(29.1) has to be visualized more closely, as it plays a major role in the longitudinal magnetic recording. The difference of two arctangent functions is nothing more than the angle θ subtended by the gap at a given location of (x, y) , where the value of field is required, which is illustrated in Figure 29.2.

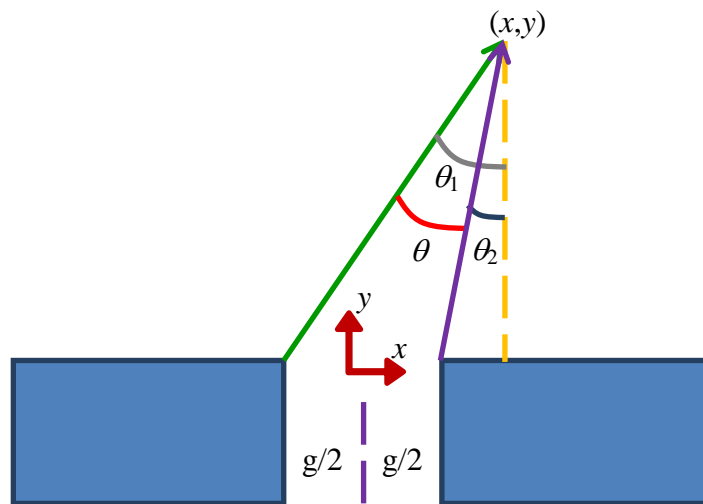


Figure 29.2: Karlqvist head field in terms of an angle.

Hence, the x -field equation in the eqn.(29.1) can be written as

$$H_x(x, y) = \frac{H_g}{\pi} \theta \tag{29.2}$$

where $\theta_1 = \tan^{-1} \left(\frac{x+g/2}{y} \right)$ and $\theta_2 = \tan^{-1} \left(\frac{x-g/2}{y} \right)$ and $\theta = \theta_1 - \theta_2$.

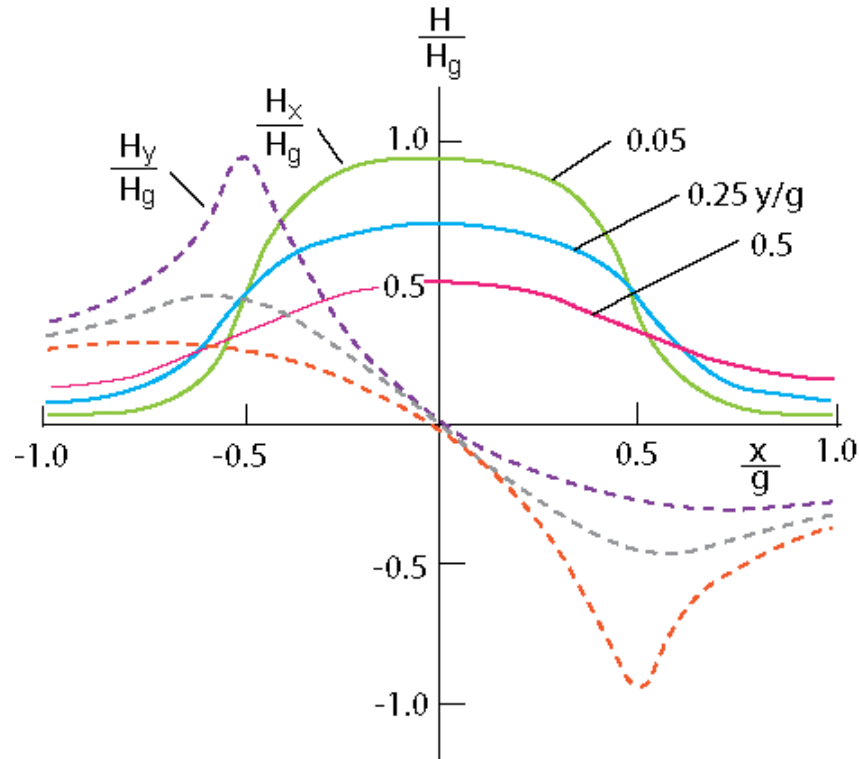


Figure 29.3: Normalized x and y components of the head field.

Using the above equation, the variations of H_x and H_y can be displayed, as shown in Figure 29.3 along the x and y axes. The value of H_x is the maximum when the angle θ is the largest. The normalized values, the x -axis values are divided by the gap g and the field along x and y axes are divided by H_g , are displayed to make the universal plot, independent of g and H_g values. It is clearly seen from the figure that the field exhibits maximum value along the vertical axis and also shown growing larger with decreasing the values of y . Similar the field along y direction is zero near the gap center, but shows peaks at some distance from the center.

The important understanding from the above equation is how the horizontal component of the head field changes with increasing the distance away from the head tip. The relation for the variation of head field with increasing y can be calculated by setting x value as zero in eqn.(29.1). Hence, the eqn.(29.1) turns out to be,

$$H_x(0, y) = \frac{2H_g}{\pi} \tan^{-1} \left(\frac{g}{2y} \right) \quad (29.3)$$

$$H_y(0, y) = 0$$

It is clear from the figure 29.4 that the horizontal component of the x field at a given y value decreases sharply with decreasing the head gap. If the head gap tends to zero, then there is no x field available for writing the medium. Note that the assumption of head gap zero is the single pole head used for perpendicular magnetic recording.

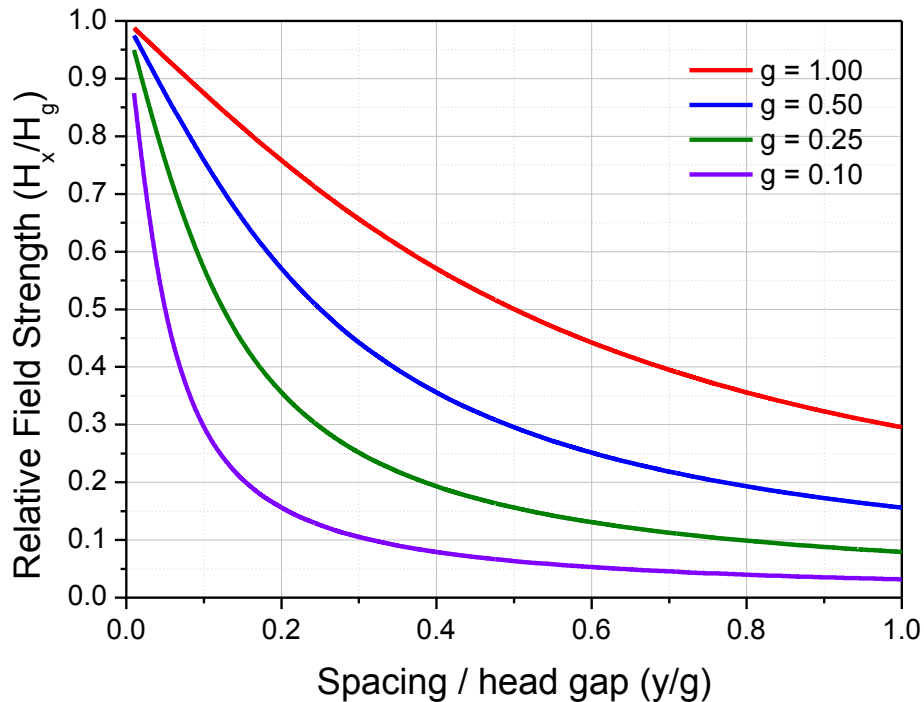


Figure 29.4: Variation of peak head field as a function of the ratio between the spacing and head gap (with different head gap values).

Problem on Head field Calculations:

1. Calculate the current required to produce a head gap field suitable to write a medium having the average coercivity of 1600 Oe. The head gap is 400 nm and the flying height is 100 nm. Assume that the medium thickness is small compared to the flying height.

Solution:

A field H_x is equal to 2.5 times of the coercivity of the medium is required for proper writing. Hence $H_x = 1600 \times 2.5 = 4000$ Oe. Now, $y/g = 100/400 = 0.25$. For the value of $y/g=0.25$, the H_x/H_g is given as 0.7. Therefore, the gap field is $H_g=H_x/0.7 \rightarrow 4000 /0.7 \rightarrow 5700$ Oe (454 kA/m).

The magnetomotive force required to produce the head field is given as $H_g \times g = 454$ kA/m $\times 400 \times 10^{-9} \rightarrow 182$ mA for a single turn head. In case of 20 turn head, the current requires is around 9mA.

References:

- [1]. R.M. White, Introduction to Magnetic Recording, IEEE Press, New York, 1985, Chapter. 3.3.
- [2]. K.G. Ashar, Magnetic disk drive technology: Heads, Media, Channel, Interfaces, and Intergration, IEEE Press, New York, 1997.

Module 4: Aspects of Magnetic Recording Head

Lecture 30: Perpendicular Head Fields

Since the size of the magnetic granular particles in the existing CoCrPt based recording media approached the super-paramagnetic limit to the areal densities beyond 100 Gbits/inch², the data storage industry is finally coming into terms with the reality, which suggest that the areal density in cutting-edge laboratory demonstration systems is limited by thermal instabilities in the longitudinal magnetic media [1]. On the other hand, the high areal density demonstrations of perpendicular recording clearly demonstrate the strong interest of the data storage industry in this alternative technology [2-4]. Compared to the conventional longitudinal recording mode, it is believed that perpendicular recording is capable of deferring the superparamagnetic limit to a substantially higher areal density due to the thinner recording layer and/or the use of a soft underlayer (SUL). Although there are many questions related to the implementation of the perpendicular magnetic recording is unclear, in this lecture, our motivation is to demonstrate various possible modes of writing the perpendicular recording medium using the perpendicular fields from the head and the understanding of the perpendicular field from the head for maximizing the achievable areal density.

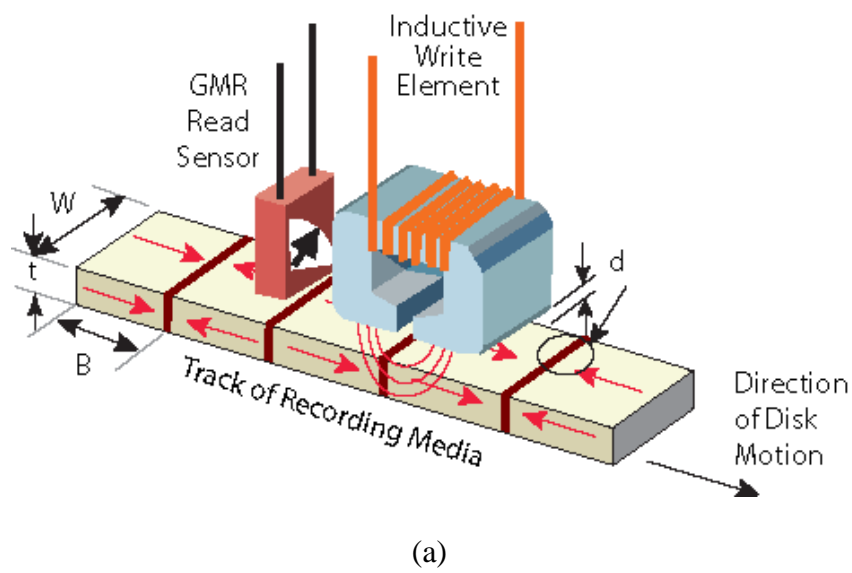
Various methods of Perpendicular Recording:

Basically, there are two modes of perpendicular recording: (1) The first method utilizes a regular ring head for recording onto a single-layer perpendicular medium without any soft underlayer (SUL), as shown in Figure 30.1a. This mode is almost similar to the conventional longitudinal mode. (2) The second method utilizes a single pole head for recording onto a double-layer perpendicular medium consisting of a recording layer and a SUL, as shown in Figure 30.1b [5]. We shall now discuss the various modes of writing in detail.

A Ring Head and a perpendicular medium without a SUL:

This method of writing involves a conventional longitudinal ring head and a recording medium without any SUL. We have already discussed the generation of head field using typical ring head in the earlier lecture based on the Karlqvist's two-dimensional (2D) model [6,7]. Since the track width of the recording bits reduces drastically for obtaining the high areal densities, the field calculation using the 2D model may not provide sufficient accuracy. Therefore, the results of 3D calculations [8] made with the boundary element model (BEM)-based commercial field solver Amperes will be discussed briefly. For detailed understanding of the head fields, the readers may go through the articles specifically on the writing process of the perpendicular magnetic recording.

The gap length dependence of the field and trailing pole thickness dependence of the field are the two of the factors controlling the field required for writing perpendicular medium. As we have seen in our earlier discussion in Lecture 29 (see Figure 29.4) that as the gap length decreases the horizontal component of the field decreased largely and longitudinal field component is fairly well localized in the gap region. In this case, the field near the trailing edge of the gap produces recording as shown in Figure 30.2. As a result, by having the gap considerably small, a fairly sharp field profile and large areal densities can be generated. With increasing the gap length, the efficiency of the head is proportional to the dependence of the saturation current on the gap length. If we assume that the saturation current is defined as the current to produce the field of $2\pi M_S$ at the center of the gap, then the current required to produce such field increases with increasing the gap length.



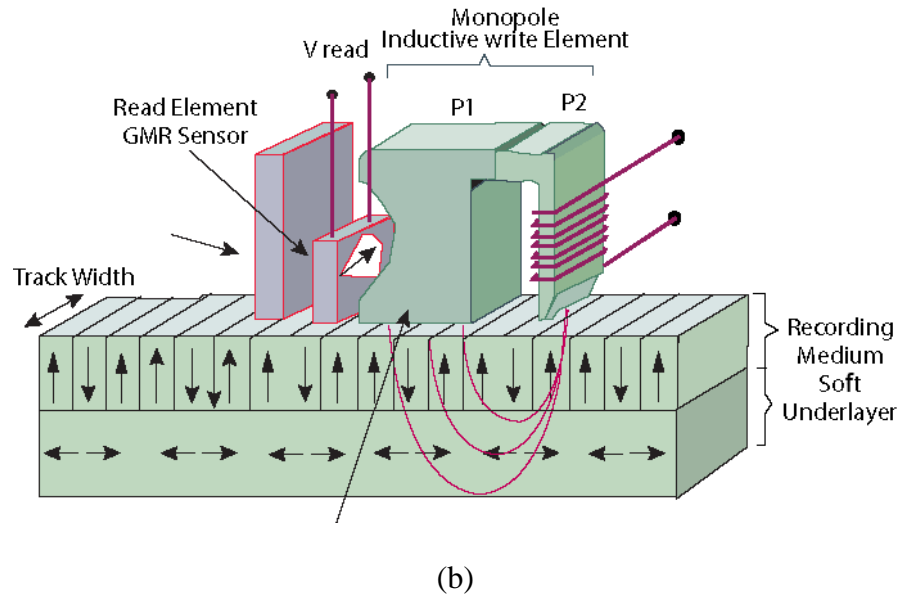


Figure 30.1: Schematic drawing of a perpendicular recording using (a) ring head, and (b) single pole head.

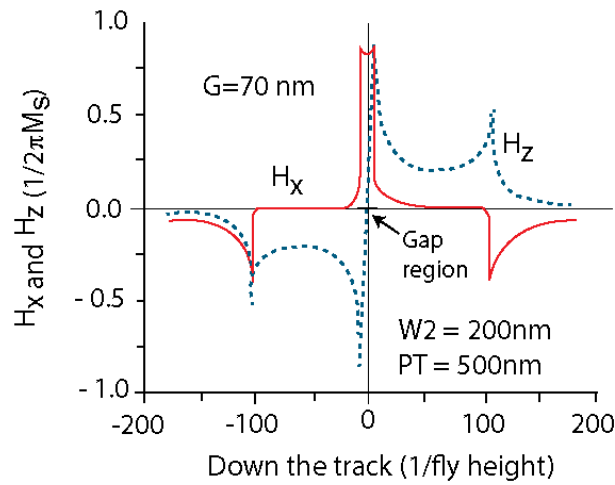


Figure 30.2: Longitudinal and perpendicular field components versus the distance down the track for a ring head with a track width of 200 nm, a pole thickness of 500 nm at 70 nm gap length [8].

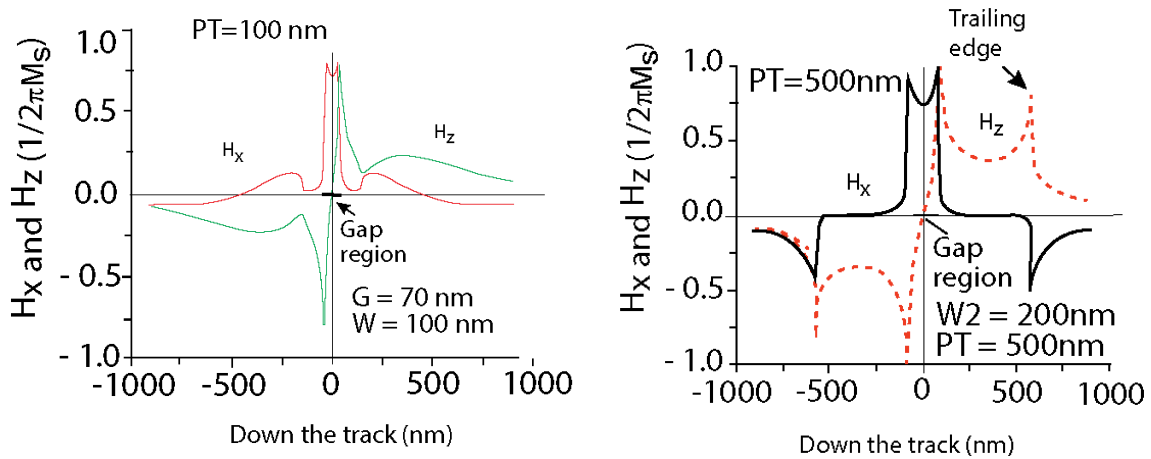


Figure 30.3: Longitudinal and perpendicular field components versus the distance down the track for a ring head with a trackwidth of 100 nm, a gap length of 70 nm and at different pole thickness [8].

Similarly, the perpendicular component of the field increases with increasing the trailing pole thickness more than by a factor of three, as shown in Figure 30.3. Note that the longitudinal component of the field does not change largely with increasing the pole thickness. Nevertheless, the written field in a recording medium without SUL obtained by using ring head is similar to the longitudinal mode and the maximum field never exceeds beyond $2\pi M_S$.

A Single pole head and a perpendicular medium with a SUL:

As shown in the Figure 30.1b, this mode of writing has a single pole head and medium with a SUL. The flying height in this arrangement is much higher than the one in the longitudinal recording so that the magnetic flux can be forced to flow through the SUL rather than leaking through the gap regions, which helps to enhance the perpendicular component of the magnetic field at least by 2 times.

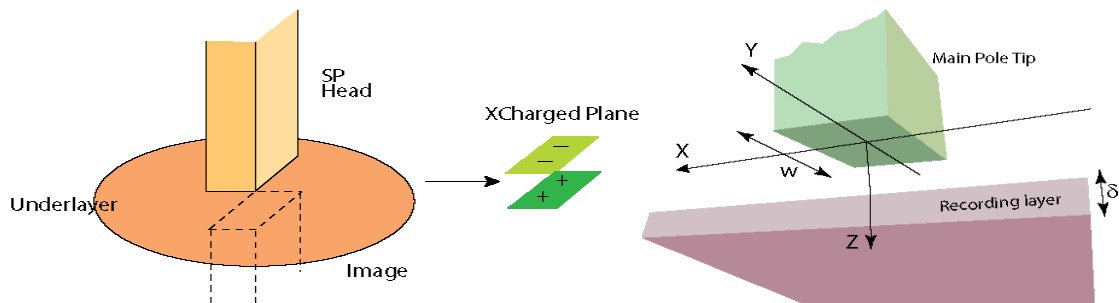


Figure 30.4: (a) Single pole head with its image, equivalent to two charged planes. [9], (b) Location of the origin of the coordinate system utilized in the calculation [8].

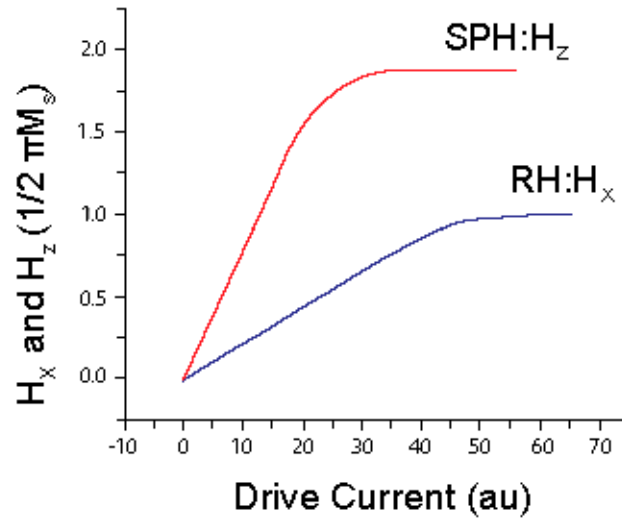


Figure 30.5: Variation of the horizontal and perpendicular component of the fields as a function of drive current for a ring head and single pole head [8].

The calculation of the head field can be done by assuming that the single pole head as an infinitely long vertical magnetic bar with the finite cross section dimensions, W and thickness T , with its magnetization aligned along the vertical axis. In such cases, the magnetic field components can be calculated using the equivalent charge model (see Figure 30.4), as demonstrated by Okuda et al [9]. It has been shown that the head field of single pole head is equivalent to that of single pole head with its image, because the boundary conditions, such as that the potential at the surface of the underlayer is equal to zero, are satisfied [10]. Figure 30.4a shows the presence of the SUL, which can be taken into account through the magnetic image model, while Figure 30.4b shows the origin of the coordinate system which is at the center of the pole tip air-bearing surface with the vertical axis, Z , directed downward. In addition, the spacing between the real and image heads is equal to the recording layer thickness plus the separation between the recording layer and the SUL. The sum of the two fields gives the total recording field. As shown in Figure 30.4, the advantage of perpendicular recording from the mirror image model is that due to the SUL the effective number of the current sources is doubled and hence the perpendicular recording needs approximately only half as much current to generate the same magnetic field in the effective gap, as compared to an equivalent longitudinal recording (see Figure 30.5). Note that the linear region slope for the single pole head is almost four times as large as the linear region slope for the ring head and if recorded on

media with the same coercivity field, the saturation current for a perpendicular system should approximately be four times as less as it is for an equivalent longitudinal system.

References:

- [1]. S. H. Charap, P.-L. Lu, Y. He, IEEE Trans. Magn **33** (1), 978 (1997).
- [2]. MRS Bulletin, p. 387, May 2003.
- [3]. S. Iwasaki, IEEE Trans. Magn. **39** (4), 1868 (2003).
- [4]. A. S. Hoagland, IEEE Trans. Magn. **39** (4), 1871 (2003).
- [5]. D.A. Thompson, J. Magn. Soc. Japan **21**, S2, (1997) 9.
- [6]. O. Karlqvist, Trans. Roy. Inst. Technol., Stockholm, **86**, 3-27 (1954).
- [7]. R.M. White, Introduction to Magnetic Recording, IEEE Press, New York, 1985, Chapter.3.
- [8]. S. Khizroev, D. Litvinov, J. Appl. Phys. 95 (2004)4521.
- [9]. K. Okuda, K. Sueoka, and K.G. Ashar, IEEE Trans Magn 24 (1988) 2479.
- [10]. S. Satake et al, Tech. Report of IECE, MR 77-26 (1977) 33.

Quiz:

- (1) What is magnetoresistance?
- (2) What are the different types of magnetoresistance explored for read head applications?
- (3) What is anisotropic magnetoresistance? How does the resistance vary in AMR elements?
- (4) What is giant magnetoresistance? How does the magnetoresistance vary with the interlayer thickness?
- (5) What is spin valve structure?
- (6) How does the GMR ratio defined in the spin valve structure?
- (7) What is the tunnelling magnetoresistance?
- (8) Does TMR depend on the polarization of the electrodes?

- (9) What are the parts available in Disk drive and describe their functions?
- (10) How does the head field from the write head vary with the distance?
- (11) What are the different types of recording available in the perpendicular recording mode?
- (12) What are advantages of perpendicular recording mode in comparison with the longitudinal recording?